AD-A162 689 ANALYSIS AND EXPERIMENTS ON INTERLAMINAR FRACTURE TOUGHNESS IN RESIN MATR (U) GEORGIA INST OF TECH ATLANTA SCHOOL OF AEROSPACE ENGINEERING 1/1

UNCLASSIFIED L W REHFIELD ET AL JUL 85 AFOSR-TR-85-1075 F/G 11/4 NL

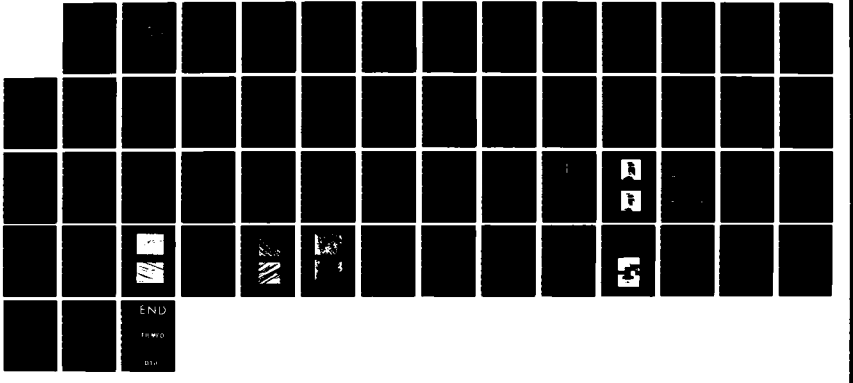

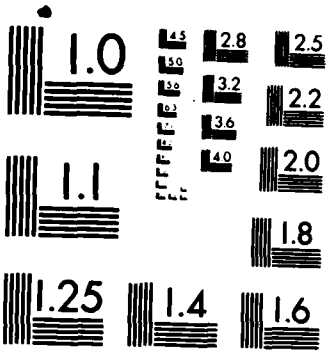


MICROCOPY RESOLUTION TEST CHART
NATIONAL BUREAU OF STANDARDS-1963-A

(2)



# ANALYSIS AND EXPERIMENTS ON INTERLAMINAR FRACTURE TOUGHNESS IN RESIN MATRIX COMPOSITES




Lawrence W. Rehfield, Erian A. Armanios and Ambur D. Reddy
School of Aerospace Engineering
Georgia Institute of Technology
Atlanta, Georgia 30332

Final Scientific Report
1 January 1983 - 14 April 1985
AFOSR Grant No. 83-0056

July 1985

UNCLASSIFIED

SECURITY CLASSIFICATION OF THIS PAGE

## REPORT DOCUMENTATION PAGE

| | |
|---|---|
| 1a. REPORT SECURITY CLASSIFICATION: UNCLASSIFIED | 1b. RESTRICTIVE MARKINGS: ADA-162 689 |
| 2a. SECURITY CLASSIFICATION AUTHORITY | 3. DISTRIBUTION/AVAILABILITY OF REPORT: UNLIMITED Approved for public release; distribution unlimited. |
| 2b. DECLASSIFICATION/DOWNGRADING SCHEDULE | |
| 4. PERFORMING ORGANIZATION REPORT NUMBER(S) | 5. MONITORING ORGANIZATION REPORT NUMBER(S): AFOSR-TR- 85-1075 |
| 6a. NAME OF PERFORMING ORGANIZATION: Georgia Institute of Technology; 6b. OFFICE SYMBOL (If applicable) | 7a. NAME OF MONITORING ORGANIZATION: Air Force Office of Scientific Research/NA |
| 6c. ADDRESS (City, State and ZIP Code): School of Aerospace Engineering, Atlanta, Georgia 30332 | 7b. ADDRESS (City, State and ZIP Code): Bolling Air Force Base, DC 20332 |
| 8a. NAME OF FUNDING/SPONSORING ORGANIZATION: AFOSR; 8b. OFFICE SYMBOL (If applicable): NA | 9. PROCUREMENT INSTRUMENT IDENTIFICATION NUMBER: AFOSR-83-0056 |
| 8c. ADDRESS (City, State and ZIP Code): Bolling Air Force Base, DC 20332 | 10. SOURCE OF FUNDING NOS. |

| PROGRAM ELEMENT NO. | PROJECT NO. | TASK NO. | WORK UNIT NO. |
|---|---|---|---|
| 61102F | 2307 | B2 | |

11. TITLE (Include Security Classification): Analysis and Experiments on Interlaminar Fracture Toughness in Resin Matrix Composites

12. PERSONAL AUTHOR(S): Lawrence W. Rehfield, Erian A. Armanios and Ambur D. Reddy

| 13a. TYPE OF REPORT | 13b. TIME COVERED | 14. DATE OF REPORT (Yr., Mo., Day) | 15. PAGE COUNT |
|---|---|---|---|
| Final Scientific | FROM 1/1/83 TO 4/85 | July 1985 | 53 |

16. SUPPLEMENTARY NOTATION

| 17. COSATI CODES | | | 18. SUBJECT TERMS (Continue on reverse if necessary and identify by block number) |
|---|---|---|---|
| FIELD | GROUP | SUB. GR. | DELAMINATION, FRACTURE TESTING, FRACTURE, INTERLAMINAR FRACTURE, MODE II FRACTURE, COMPOSITE MATERIALS, COMPOSITE STRUCTURES |
| | | | |
| | | | |

19. ABSTRACT (Continue on reverse if necessary and identify by block number)

This final report summarizes the objectives, accomplishments and proposed new direction of research on mode II interlaminar fracture in resin matrix composites. The work was performed during the period 1 January 1983-14 April 1984. A mode II interlaminar fracture specimen, test and analysis method for interpreting results have been successfully developed and demonstrated for the AS4/3502 material system. Experimental data have been obtained under both net tensile and compressive loading. Of considerable importance are the findings that

Cont'd

| 20. DISTRIBUTION/AVAILABILITY OF ABSTRACT | 21. ABSTRACT SECURITY CLASSIFICATION |
|---|---|
| UNCLASSIFIED/UNLIMITED ☑ SAME AS RPT ☑ DTIC USERS ☐ | UNCLASSIFIED |

| 22a. NAME OF RESPONSIBLE INDIVIDUAL | 22b. TELEPHONE NUMBER (Include Area Code) | 22c. OFFICE SYMBOL |
|---|---|---|
| Dr Amos | (202) 767-4935 | NA |

DD FORM 1473, 83 APR EDITION OF 1 JAN 73 IS OBSOLETE.

UNCLASSIFIED

SECURITY CLASSIFICATION OF THIS PAGE

Abstract Cont'd

1) the AS4/3502 material system shows increasing resistance to crack growth in tension, 2) interlaminar fracture under compression is a totally unstable process, and 3) tension and compression behaviors are considerably different. The findings and the conclusions that are drawn from them point to new, promising directions.

Complementary experiments on low cycle fatigue in tension and compression and on mode I suppression in tension have been performed. The former basically confirm the static findings. The latter illustrate the potential effectiveness of mode I suppression technology and help to clarify mixed mode fracture.

## INTRODUCTION

The work described herein was performed at the School of Aerospace Engineering, Georgia Institute of Technology during the period 1 January 1983 - 14 April 1985. Professor Lawrence W. Rehfield was the Principal Investigator. The research objectives were:

1. Develop a mode II interlaminar fracture specimen design and test;
2. Develop efficient means of analyzing and understanding the results; and
3. Design the test so that it may be performed under both net tensile or compressive loading.

All of the above objectives were met within the first thirteen and one-half month period. In order to accomplish them, it was necessary to develop a suitable method of analysis appropriate to the design process, design and fabricate test specimens and perform definitive experiments. The experimental results confirm that the specimens and tests perform as designed. Of great importance are the findings that (1) the AS4/3502 material system shows increasing resistance to crack growth in tension, (2) interlaminar fracture under compression is a totally unstable process, and (3) tension and compression behaviors are considerably different. These findings and the logical conclusions that are drawn from them pointed to new,

promising directions for further inquiry which were pursued during the remaining time.

The findings prompted us to move in the following new directions:

1. Perform exploratory fatigue tests under both mean tension and mean compression;
2. Study the effect of peel stress or mode I suppression by applying clamping pressure to the lap of a specimen and testing it in static tension;
3. Perform thorough failure analyses using enhanced radiography, ultrasonic scanning, scanning electron microscopy and optical microscopy to determine and characterize the damage states and facilitate isolation of the fracture mechanism(s).

This complementary work aided enormously in crystalizing the conclusions drawn from the primary investigation. Together the studies provided the basis for a number of important new findings on interlaminar fracture.

## SUMMARY OF ACCOMPLISHMENTS

### Foundation Provided by Previous Work

The present research in interlaminar fracture had its origin in the development of new structural models under two previous AFOSR grants, 81-0056 and 82-0080, which permitted prediction of interlaminar stresses in composites and other behavioral characteristics by elementary means. It was natural to harness this potential for design analysis of composite specimens. Earlier analytical work, which was

completed and published during the current period and which provided the foundation for the design analysis required in the present research, appears in Accomplishments (1-5, 9). Of importance to the experimental phase of the research are the design analysis method developed in Accomplishment (10), the experimental experience with compression testing in Accomplishment (6) and the experiments on compressed panels with prescribed delaminations reported in Accomplishments (7,8).

The purpose of citing the above is two-fold: (1) these accomplishments provided the background and the basis for the present research and (2) effort was expended during the present grant period in order to complete them and bring them to publication.

Overview of the Research

As indicated in the Introduction, the research objectives were met by developing a suitable method of analysis for use in specimen design, designing and fabricating specimens, and performing the experiments. A complete account of the primary investigation appears in Accomplishment (12). Results of the complementary work appear in Appendix II, which is an extended abstract of what will be presented in Accomplishment (19). A readily available reference for the analysis methodology and the specimen design is Accomplishment (11).

The experimental approach, results and thorough discussion of results obtained in the primary investigation are

included herein as Appendix I. This is the manuscript associated with Accomplishments (16, 30).

The project in its entirety is contained in Accomplishment (12) and the two Appendices of this report. It is noteworthy that Dr. R.R.Valisetty's thesis, Accomplishment (2), and Dr. E.A. Armanios' thesis, Accomplishment (12), have each been recognized as the Outstanding Ph.D. Thesis in Engineering at the Georgia Institute of Technology for 1983 and 1985, respectively.

Modeling, Analysis and Design

The key to developing a successful experimental method is an effective design analysis methodology and practical specimen design criteria. The desired objective is to be able to test under both net tensile and compressive loads, test both statically and in a fatigue spectrum and produce interlaminar cracks in a specimen so that the specimen appears of infinite extent and the notch which serves as the origin of the crack appears isolated. This was accomplished.

The analysis methodology continues to evolve. It has been documented in Accomplishments (10-13, 15, 16). A transition has been accomplished from beams to plates[2,5] to composite laminates[1,3] to the present state of sublaminate scale[2,10,14,13]. Originally, a ply-by-ply approach to sublaminate analysis was adopted[2,14]. While extremely effective in the limited context within which it was applied - - the finite-width free edge specimen in tension, it is

cumbersome and appears somewhat impractical for widespread application. Consequently, an approximate engineering approach has been applied in the present work which treats whole sublaminate elements - - groups of plies - - as continuous laminates. The novel feature is the fact that the laminate model incorporates physical modes of deformation normally not present in engineering theories - - transverse shear strain, transverse normal strain and section warping.

The specimen configuration, a double cracked-lap-shear (DCLS) design, and design requirements appear in Appendix I.

The authors believe that perhaps the most important result of long-term significance that this research has spawned is the modeling technology.

Experimental Method and Results

The experimental method used in testing specimens under net tensile and compressive forces is fully described in Appendix I. The compressive test method is similar to the tensile but also requires the use of a fixture to provide alignment, stabilization of the tabbed ends of the specimen and flat, parallel loading surfaces. A summary of test results appears in Table 3, Appendix I.

There are two very important findings from the static experiments. The first is that under net tensile loading interlaminar fracture is a three stage process - - initiation, stable growth following a nearly linear resistance curve and a tertiary unstable terminal fracture at a high

level of load. The second is that the compressively loaded specimens exhibited absolutely no stable crack growth. Failure occurred in a catastrophic, unstable manner with no warning at a high level of load. Test data for two specimens, one tested in tension and the other in compression, are presented in Figure 5, Appendix I. The loads corresponding to failure by unstable fracture for these specimens are close to the same.

Complementary experiments on low cycle fatigue in tension and compression and on mode I suppression in tension are described in Appendix II. Although the number of specimens tested is small, the former suggest that fatigue behavior is quite similar to static behavior. It does not appear possible to have stable interlaminar crack growth in compression for AS4/3502 graphite/epoxy. The latter help to clarify mixed mode fracture and clearly indicate the potential effectiveness of mode I suppression technology.

A detailed discussion of the conclusions drawn from the primary work appears in Appendix I.

## ACKNOWLEDGEMENTS

Numerous persons have contributed to this research over the period of performance by providing advice, exchanging information and responding to questions. A list of them appears in Table 1. Their input has been gratefully received.

TABLE 1

CONTRIBUTORS TO THE RESEARCH

AFOSR

MAJOR DAVID GLASGOW

BELL HELICOPTER TEXTRON,INC.

WEN CHAN

GENERAL DYNAMICS

DICK WILKINS, GEORGE LAW

GLOBAL ANALYTICS,INC;

KEITH KEDWARD

LOCKHEED-GEORGIA COMPANY

HARRY ALLEN
SHERRIL BIGGERS
JOHN DICKSON
BERT FERHLE
KRIS KATHIRESAN
SAM FREEMAN

NORTHROP CORPORATION

RAVI DEO
MOHAN RATWANI

AFML

JAMES WHITNEY

NASA LANGLEY RESEARCH CENTER

WOLF ELBER
STEVEN JOHNSON
KEVIN O'BRIEN
BLAND STEIN
JOHN WHITCOMB

## ACCOMPLISHMENTS

### Publications


1. Rehfield, L.W. and Valisetty, R.R., "A Comprehensive Theory for Planar Bending of Composite Laminates," presented at the Symposium on Advances and Trends in Structural and Solid Mechanics," Computers and Structures , Vol. 16, No. 1-4, 1983,pp. 441-447.

2. Valisetty, R.R., "Bending of Beams, Plates and Laminates: Refined Theories and Comparative Studies," Ph.D. Thesis, Georgia Institute of Technology, March 1983.

3. Valisetty, R.R. and Rehfield, L.W., "A Theory for Stress Analysis of Composite Laminates," AIAA Journal , Vol. 23, No. 7, July 1985, pp. 1111-1117.

4. Yehezkely, O. and Rehfield, L.W., "A New, Comprehensive Theory for Bending and Buckling of Stiffened Plates," Israel Journal of Technology , Vol. 20, 1982, pp 233-244.

5. Rehfield, L.W.and Valisetty, R.R., "A Simple, Refined Theory for Bending and Stretching of Homogeneous Plates," AIAA Journal , Vol. 22, No. 1, January 1984, pp. 90-95.

6. Reddy, A.D., Rehfield, L.W., Haag, R.S., and Widman, C., "Compressive Buckling Behavior of Graphite/Epoxy Isogrid Wide Columns with Progressive Damage," appears in Compression Testing of Homogeneous Materials and Composites , ASTM STP 808, edited by R. Chait and R. Paperino, 1983, pp. 187-199.

7. Reddy, A.D., Rehfield, L.W. and Haag, R.S., "Effect of Large Delaminations on the Compressive Postbuckling Behavior of Laminated Composite Panels," Proceedings of the Sixth Conference on Fibrous Composites in Structural Design , Report AMMRC MS 83-2, Army Materials and Mechanics Research Center, November 1983, pp. VI-41 to VI-51.

8. Reddy, A.D., Rehfield, L.W. and Haag, R.S., "Influence of Prescribed Delaminations on Stiffness Controlled Behavior of Composite Laminates," ASTM Symposium on Effects of Defects in Composite Materials, December 13-14, 1982. Appears in Effects of Defects in Composite

Materials , edited by D.J. Wilkins, ASTM STP 836, 1984, pp. 71-83.

9. Rehfield, L.W., Prucz, J. and Murthy, P.L.N., "Influence of Hygrothermal Conditioning on the Compressive Buckling of Graphite/Epoxy Structures," Journal of the American Helicopter Society , Vol. 29, No. 2, April 1984, pp. 12-15.

10. Rehfield, L.W., Armanios, E.A. and Changli, Q., "Analysis of Behavior of Fibrous Composite Compression Specimens," Composites in the United States and Japan , edited by J.R. Vinson and M. Taya, ASTM STP 864, 1985.

11. Rehfield, L.W., Armanios, E.A. and Reddy, A.D., "Interlaminar Fracture Toughness in Resin Matrix Composites," Annual Scientific Report, AFOSR Grant No. 83-0056, April 1984.

12. Armanios, E.A., "New Methods of Sublaminate Analysis for Composite Structures and Applications to Fracture Processes," Ph.D. Thesis, Georgia Institute of Technology, December 1984.

13. Rehfield, L.W., Armanios, E.A. and Valisetty, R.R., "Simplified Sublaminate Analysis in Composites and Applications," Symposium on Advances and Trends in Structures and Dynamics, Washington, D.C., 22-24 October 1984, Computers and Structures , Vol. 20, No. 1-3, 1985, pp. 401-411.

Publications Pending

14. Valisetty, R.R. and Rehfield, L.W., "A New Approach to Interlaminar Stress Analysis," to appear in Delamination and Debonding of Materials , edited by W.S. Johnson, an ASTM STP Volume.

15. Armanios,E.A., Rehfield, L.W. and Reddy, A.D., "Design Analysis and Testing for Mode II Interlaminar Fracture of Composites," Composite Materials: Testing and Design (Seventh Conference), edited by J.M. Whitney, ASTM STP 893, 1986.

16. Rehfield, L.W., Reddy, A.D. and Armanios, E.A., "Interlaminar Fracture of Graphite/Epoxy Composites Under Tensile and Compressive Loading," presented at the ASTM Symposium on Toughened Composites, Houston, Texas, March 1985. To be published in an ASTM STP Volume.

17. Reddy, A.D., Rehfield, L.W., Weinstein, F. and Armanios, E.A., "Interlaminar Fracture Processes in

Resin Matrix Composites Under Static and Fatigue Loading," to be presented at ASTM Composite Materials Testing and Design: Eighth Symposium, Charleston, SC, 28-30 April 1986. To be published in the Proceedings, an ASTM STP Volume.

Presentations

18. Rehfield, L.W., "New Theories of Bending," Boeing Vertol Company, Philadelphia, PA, 23 February 1983.

19. Reddy, A.D., Rehfield, L.W. and Haag, R.S., "Effect of Large Delaminations on the Compressive Postbuckling Behavior of Laminated Composite Panels," 6th Conference on Fibrous Composites in Structural Design, New Orleans, LA, January 24-27, 1983.

20. Rehfield, L.W., Prucz, J. and Murthy, P.L.N., "Influence of Hygrothermal Conditioning on the Compressive Buckling of Graphite/Epoxy Composite Structures," American Helicopter Society National Specialists' Meeting on Composite Structures, Philadelphia, PA, March 23-25, 1983.

21. Valisetty, R.R. and Rehfield, L.W., "A Theory for Stress Analysis of Composite Laminates," AIAA Paper 83-0833-CP, 24th AIAA SDM Conference, Lake Tahoe, Nevada, May 204, 1983.

22. Rehfield, L.W., "Innovations in Damage Tolerance Analysis," Symposium on NDE of Criticality of Defects in Composite Laminates, Philadelphia, PA, May 23, 24, 1983.

23. Rehfield, L.W., Armanios, E.A. and Changli, Q., "Analysis of Behavior of Fibrous Composite Compression Specimens," Second U.S.-Japan Symposium on Composite Materials, NASA Langley Research Center, Hampton, VA, June 6-8, 1983.

24. Rehfield, L.W., "Innovations in Modeling of Conventional and Composite Structures,: Invited Lecture, Army Materials and Mechanics Research Center, Watertown, MA, 28 July 1983.

25. Valisetty, R.R. and Rehfield, L.W., "A New Approach to Interlaminar Stress Analysis," ASTM Symposium on Delamination and Debonding of Materials, Pittsburgh, PA, 9-10 November 1983.

26. Armanios,E.A., Rehfield, L.W. and Reddy, A.D., "Design Analysis and Testing for Mode II Interlaminar Fracture of Composites," presented at

a. Northrop Corporation, Hawthorne, CA, 27 February 1984.
b. Hughes Helicopter, Inc., Culver City, CA, 1 March 1984.
c. Army Aeromechanics Laboratory, Ames Research Center Moffett Field, CA, 5 March 1984.
d. Invited Lecture, Seminar on Matrix Resins for Composites, United Nations Industrial Development Organization and Dept. of Science and Technology, Government of India, Indian Institute of Technology, Delhi, India, 12-14 March 1984.
e. Messerschmitt-Bolkow-Blohm, Helicopter Division, Munich, West Germany, 19 March 1984.
f. Army Applied Technology Laboratory, Fort Eustis, Va, 27 MARCH 1984.
g. NASA Langley Research Center, Hampton, VA, 28 March 1984.
h. ASTM Symposium on Composite Materials: Testing and Design, Philadelphia, PA, 2-4 April 1984. Also to be published in an ASTM STP Volume of the Proceedings.
i. Boeing Vertol Company, Philadelphia, Pa, 4 April, 1984.
j. Sikorsky Aircraft, Stratford, CT, 5 April 1984.
k. Lockheed-Georgia Company, Marietta, GA, 16 April 1984.

27. Rehfield, L.W., "Damage Tolerance of Composite Airframe Structures," Invited Lecture, 21st Society of engineering Science Conference, Blacksburg, VA, 15-17 October 1984.

28. Rehfield, L.W., Armanios, E.A. and Valisetty, R.R., "Simplified Sublaminate Analysis of Composites and Applications," Symposium on Advances and Trends in Structures and Dynamics, Washington, D.C., 22-24 October 1984.

29. Rehfield, L.W., Armanios, E.A. and Reddy, A.D., "Interlaminar Fracture of Graphite-Epoxy Composites Under Tensile and Compressive Loading," Tenth Mechanics of Composites Review, 15-17 October 1984.

30. Rehfield, L.W., Reddy, A.D. and Armanios, E.A., "Interlaminar Fracture of Graphite/Epoxy Composites Under Tension and Compression," ASTM Symposium on Toughened Composites, Houston, TX, 13-15 March 1985.

31. Rehfield, L.W., "Interlaminar Fracture Toughness of Composite Laminates," Rensselaer Polytechnic Institute, Troy NY, 26 March 1985.

# APPENDIX I

Presented at the Symposium on Toughened Composites, Houston, Texas, 13-15 March 1985, to be published in the Proceedings.

# INTERLAMINAR FRACTURE OF GRAPHITE/EPOXY COMPOSITES UNDER TENSILE AND COMPRESSIVE LOADING*

Lawrence W. Rehfield, Ambur D. Reddy and Erian A. Armanios**
School of Aerospace Engineering
Georgia Institute of Technology
Atlanta, Georgia 30332
(404) 894-3067

## ABSTRACT

Interlaminar fracture of the AS4/3502 graphite/epoxy material system is investigated using a newly designed double cracked-lap-shear (DCLS) specimen and a single cracked-lap-shear (SCLS) specimen. A fundamental feature of the designed specimens is their ability to be tested under net tensile and compressive loadings. The specimens exhibit mixed-mode or mode II behavior depending on the loading direction. The specimens are designed to precipitate crack growth at a designed-in site in a gage section. In the specimen design process, overall dimensions of the specimens are selected so that local disturbances in the stress field will not interact, there is adequate length to permit crack growth, and overall buckling will not occur under compressive loading. The experimental results confirm that the specimens and tests perform as designed. It is observed that (1) the AS4/3502 material system shows increasing resistance to crack growth in tension, (2) interlaminar fracture under compression is a totally unstable process, and (3) tension and compression behaviors are considerably different. Interfacial shear stresses corresponding to failure by unstable fracture are found to correlate with short beam shear strength data. Fracture surfaces in the unstable regions from short beam shear and DCLS specimen tests exhibit similar characteristics.

KEY WORDS: composite materials, fiber-reinforced composites, composite structure, graphite-epoxy, crack propagation, delamination, fracture, scanning electron microscopy, test methods.

---

* Sponsored by AFOSR under Grant 83-0056.

** Professor, Senior Research Engineer and Research Engineer, respectively.

# INTRODUCTION

Interlaminar fracture or delamination is a primary damage mode in laminated composites. It is caused by high interlaminar stresses which are produced by local stress raisers such as holes, free edges, ply drops and other defects and discontinuities which may be manufacturing-related or service induced. Delaminations alter internal load paths and usually contribute to the ultimate failure of the structure. Interlaminar fracture toughness, which characterizes the resistance to delamination, is a key parameter in describing the damage tolerance of laminated composite materials.

In the present work, interlaminar fracture toughness of AS4/3502 graphite/epoxy material is estimated from experiments using DCLS and SCLS specimens with end tabs. The DCLS specimen analysis, design and a comparison of tension testing only with SCLS specimen were the subject of an earlier paper [1]. Characterization of specimen behavior under net tensile and compressive loading is given here. Also, an assessment of the adequacy of the DCLS as a mixed-mode specimen under tensile loading and for the study of mode II dominated behavior under compressive loading is made. This has been done by observation of delamination growth, verification of consistency of observed behavior with each test, analysis of the data and comparison with data obtained from SCLS specimen tests. Finally, a correlation between interfacial shear stresses in the DCLS specimen and the short beam shear strength data is provided. This is done by sectioning short beam specimens from undamaged zones of the failed DCLS specimens and testing them to failure in three-point bending and through comparison of fracture surfaces from the short beam and DCLS tests.

## SPECIMEN DESIGN

Specimen design is based on a simple, new analysis method described in detail in References 1 and 2. The DCLS specimen geometry and dimensions are shown in Figure 1. The number of plies in the lap and strap region is 8 and 32, respectively. The lap/strap interface is +45/-45. The lap layup is $[\pm 45/0/90]_s$ and the strap layup is $[\pm 45/0/90]_{4s}$. The specimen is made of AS4/3502 graphite/epoxy material system.

Overall dimensions of the specimens are the result of a parametric study in which the material properties are those of AS4/3502 graphite/epoxy and the end tabs are made of woven fiberglass. The optimum number of plies and specimen dimensions were determined based on the following design conditions:

1. Preventing overall buckling.
2. Initiating a crack at lap/strap juncture first.
3. Providing an adequate length to monitor crack growth.
4. Ensuring no interaction between stress boundary layers at the tab/lap, tab/strap and the lap/strap regions.
5. Minimizing nesting effects.

## SPECIMEN FABRICATION

A single panel was fabricated by the Lockheed-Georgia company and inspected for quality using standard aerospace industry practice before sectioning into thirteen test specimens. During layup, a folded Kapton film was placed at the end of the lap/strap interface to initiate a delamination under subsequent loading.

In order to provide a base for comparison, ten SCLS specimens were fabricated using the same manufacturing procedure. The specimens are made of the same material and total number of plies as the DCLS specimens. The lap/strap

interface is +45/-45. The lap layup is $[\pm 45/0/90]_s$ and the strap layup is $[\pm 45/0/90]_{5s}$.

The specimens are designated as follows: the first two letters denote double lap (DL) or single lap(SL), the following digit indicates the specimen number. "T" in parentheses denotes tension and "C" compression. For example, DL-3(T) denotes the third double lap specimen tested in tension.

## EXPERIMENTAL PROCEDURE

The static tension tests on the DCLS specimens were performed on a displacement controlled Baldwin screw-type testing machine. The specimens were carefully positioned and the tab ends were tightly held between serrated grips. Load was applied at a displacement-control rate of 0.01 inches per minute. Two techniques were tried to measure the crack growth in the specimen. The first method involved visual observation of the cracks on the white painted (typewriter correction fluid) specimen edge [3]. In the second method, a sheet of photoelastic material was bonded on each of the surfaces of the specimen lap portion [4]. Isochromatic fringes develop at the crack front as a result of the high strain gradient in that vicinity when the specimen is loaded. These fringes were tracked through the analyzer of a reflection polariscope to locate the crack front. By comparison, the edge cracks observed from the first method did not correspond to the averaged crack length of the curved crack front observed by the second method. This was because the crack fronts were irregular regardless of the care exercised in initially aligning the specimen. Hence, the first method was considered unreliable and was abandoned. The second method was used on all the specimens due to its simple and direct nature in monitoring the crack front. Also, the isochromatic fringes served to check initial uniformity of the applied load on the specimen. The specimen was also instrumented with a custom-built linear

variable differential transformer (LVDT) displacement transducer based extensometer to measure its compliance.

The specimen was loaded continuously and the front and back cracks on both sides were followed through separate polariscopes. At a certain critical load, the first threshold of the crack growth occurred at the lap/strap juncture and it grew beyond the Kapton film. With crack growth, the specimen stiffness is reduced resulting in a load drop. The machine was stopped whenever crack growth was observed and the extent of propagation recorded together with the load. The crack growth was initially stable but intermittent on the two fronts with one crack trying to maintain parity with the other. During this phase, crack growth was possible only under increasing load. The crack front was not planar and it curved forward at the specimen edges. Some Poisson effects are inevitable due to the difference in constraint in the unloaded lap and the loaded strap and the free edges composed of dissimilar plies. This explains the delamination front curving forward at the specimen edges. The specimen failure occurred finally with both the cracks growing in an unstable manner. The load value corresponding to this event was recorded. In general, there was no crack wandering through the plies. Pictures of the isochromatic fringes before the initial crack propagation and during the stable crack growth phase are presented in Figures 2 and 3.

Altogether, three DCLS specimens were tested under net tensile loading. Crack wandering was not noticeable and failed specimens were indistinguishable from the untested ones to the unaided eye. The situation is different for the SCLS specimens. A procedure similar to the DCLS specimen testing was used. However, the SCLS specimens exhibited the following problems:

1. The first crack did not always initiate at the lap/strap juncture;
2. Multiple, isolated cracks occurred and sometimes grew in opposite directions;

3. The crack at lap/strap juncture wandered.

The compressive test method is similar to the tensile test, but requires the use of a fixture to provide alignment stabilization of the tabbed ends of the specimen and flat, parallel loading surfaces. A comparison between the fixtures used in tension and compression testing is shown in Figure 4. No crack growth was observed prior to a single, unstable, catastrophic fracture event which fails the specimen. Also, loads corresponding to failure by unstable fracture under tension and compression testing were close to the same. Typical tension and compression behavior are illustrated in Figure 5 where the absolute value of the applied loading is plotted against crack length.

Altogether twelve specimens have been tested, six double lap and six single lap specimens. Three of each were tested under tensile loading while the other three were tested under compressive loading. The failed specimens were sectioned and the fracture surfaces were observed under a scanning electron microscope. The fracture surfaces in the unstable regions for specimens tested under tensile and compressive loadings were found similar. This and the fact that the loads corresponding to failure in both cases are close to the same may imply that the unstable fracture processes at high loads can be described by strength-related parameters. A preliminary assessment of this issue has been made by sectioning short beam specimens from undamaged zones of the failed DCLS specimens. Altogether, eight short beam specimens with a $[\pm 45, 0, 90]_{6s}$ quasi-isotropic balanced symmetric layup, have been prepared. These short beam specimens have been tested to failure in three-point bending. The schematic of the short beam shear tests is shown in Figure 6. Similar to the DCLS and SCLS specimens in compression, no crack growth was observed prior to a single, unstable, catastrophic fracture event which fails the short beam specimen. Two off-center interlaminar symmetric cracks were observed to initiate and grow catastrophically in all tests.

## RESULTS AND DISCUSSION

During tension testing the crack growth data, taken at five locations along the width of the specimen and from both the front and back faces, was averaged to obtain a resultant crack length corresponding to each load. To eliminate the edge effects, crack length values at the edges were discarded in the averaging process. The data from the three double cracked-lap-shear specimens, tested under tensile loading, are presented in Figure 7. Numbers 1, 2 and 3 in this figure correspond to data points from specimens DL-1(T), DL-2(T) and DL-3(T), respectively. The data are plotted together as the specimens were generated from the same parent panel.

The load vs. crack growth data appears in Figure 7. The data show that there is a consistent increase in the critical load with crack length. In this context, the load required to cause a crack extension is defined as critical load. A linear least squares fit through the data is also plotted in Figure 7. The linear fit equation is provided in Reference 1. There are three phases in the resistance curve. A starting region corresponding to the onset of crack growth, an intermediate region corresponding to stable crack growth and a final or failure region of unstable crack growth. The fit shown in Figure 7 describes the stable crack growth region.

Delamination crack growth is usually characterized by the strain-energy release rate. For linear, elastic material behavior [5] and the proposed specimens geometries

$$G = P^2(dC/da)/2b \qquad (1)$$

where P is the applied load, C is the specimen compliance, a is the crack length and b is the specimen width. The critical strain energy release rate, $G_c$, is obtained by substituting the critical load $P_c$ for P in Equation (1).

The results on the three DCLS specimens tested in tension are summarized in Table 1. The critical loads that initiated the crack growth beyond the Kapton film and the corresponding energy release rates are listed, along with the rate of change of compliance with crack extension. The total critical strain energy release rate is $G_c$. The small amount of scatter in the observed critical load data may be attributable to the design and testing approach chosen. The specimen geometry and symmetry virtually eliminate geometrically nonlinear effects and the $\pm 45^{o}$ interface minimized nesting and the resulting crack wandering. Observation of the crack front by means of the photoelastic coating provided complete characterization across the width of the specimen and helped accurately determine the initial and subsequent crack growths with loading. This situation is different from the problems encountered in SCLS specimen testing. Crack wandering and the presence of multiple cracks growing in opposite directions contributes to the data scatter appreciably. This situation is illustrated in Figure 8 where the load versus crack extension data from two SCLS specimens are plotted. Number 2 and 3 in this figure correspond to data points from specimens SL-2(T) and SL-3(T), respectively. The crack extension data in Figure 8 are based on visual observation of the cracks on the white painted specimen edge. This crack tracking method (based on edge crack information only) may contribute to the data scatter. In the third tension test, the photoelastic coating method was tried for the first time on the SCLS specimen SL-4(T). The crack front was tracked through the analyzer of a reflection polariscope and the loads corresponding to initial crack growth and final unstable growth only were recorded. In the subsequent tests, graduated tapes were glued to the photoelastic coating in order to help in measuring crack front location with loading during the stable phase of crack growth.

The data in Figure 8 show that there is a consistent increase in the critical load with crack length. Among polynomial curve fits through this data, the linear

fit corresponds to the least standard deviation. The linear fit shown in Figure 8 describes the stable crack growth region. The linear fit equation is provided in Reference 1.

The results on the three SCLS specimens tested in tension are summarized in Table 2. The critical loads that initiated the crack growth beyond the Kapton film and the corresponding energy release rates are listed, along with the rate of change of compliance with crack extension. The total critical strain energy release rate is $G_c$. The standard deviation in the critical load values in Table 2 is 16,600 N (3,732 lbs) for a mean value of 50,649 N (11, 387 lbs). The standard deviation in the critical load values for the DCLS specimens in Table 1 is 1,993N (448 lbs) for a mean value of 50,618 N (11, 380 lbs). The amount of scatter in the observed critical load data may be attributable to the SCLS specimen and the crack tracking method. Similar scatter were found in SCLS specimen testing by other investigators [3,6].

A summary of test results appears in Table 3. The nominal strain is $\varepsilon$. The loads corresponding to failure, $P_f$, by unstable fracture in tension or compression are close to the same. For the SCLS specimens, the mean value of $P_f$ in tension is 82, 021 N (18,440 lbs), while the corresponding value in compression is 80, 567N (18,113 lbs.). For the DCLS specimens, the mean value of $P_f$ in tension and compression is 71, 435 N (16, 060 lbs) and 74,073 N (16, 653 lbs), respectively. The results in Table 3 are predicted based on a measured value of Young's modulus ($E_{effective}$) of 50.332 GPa (7.300 Msi). Its theoretical estimate is 53.517 GPa (7.762 Msi).

Typical photomicrographs of a fracture surface immediately after the Kapton film in the stable region and in the unstable region of crack growth are presented in Figures 9 and 10. The stable region corresponds to position 1 in Figure 11 while the unstable position corresponds to position 4. A comparison of the general features of the photomicrographs in Figures 9 and 10 indicates that crack growth in the unstable region occurs at a much higher speed than the corresponding

growth in the stable region. The fracture surface in the stable growth region appears to have predominantly high matrix deformation with lacerated resin bands and matrix cracks. These are believed to correspond to the stop-start regions of the load dependent crack fronts observed. The surface reflects "hackles" which are characteristic of matrix cleavage failure. The unstable crack growth region shown in Figure 10 is characterized by a relatively smooth surface with a small amount of fiber pull out and breakage. Striations are observed throughout the fiber pull-out region. This is characteristic of a shear failure.

A comparison of the fracture surfaces in the unstable region for tensile and compressive loading, appears in Figures 12 and 13, respectively. These are photomicrographs from the lap portion of the specimen. The fracture surfaces in both cases exhibit similar features characterized by little matrix deformation with minor fiber pull out and breakage. Striations are observed throughout the fiber pull out region on both surfaces.

A comparison of interlaminar shear data obtained from the DCLS fracture test and the short beam three point bending test is provided in Table 4. The digit following the specimen code in the short beam test data denotes the short beam specimen number. For example DL-8(C)-3 is the third short beam specimen sectioned from the double lap specimen number eight tested in compression. The maximum shear stress in the short beam were estimated based on the failure load data and a simple lamination theory [2]. Difficulties with estimating shear stresses using the simple ASTM standard method [7] have been highlighted by Whitney[8] as the test method may not yield interlaminar failures. In the present case, however, the geometry of the tested short beams yielded interlaminar failure and individual ply properties and stacking sequence effects on shear stress evaluation were considered. Failure load data and maximum shear stress appear in Table 4.

Also appearing in Table 4 are shear stress values obtained from the design analysis [2] for the actual measured values of failure load. Since the interlaminar shear stress gradient is very steep near the crack tip, which, in fact, implies singular behavior, numerical values in this location are not reliable. For this reason, the values appearing in Table 4 have been obtained by evaluating the shear stress at the location corresponding to zero peel stress in the appropriate model prediction. This is a simple way of estimating the distance away from the crack tip that the singular characteristics have decayed. Thus, a reasonably stable and meaningul limiting value of shear stress can be defined in this manner. The mean values predicted by two analytical models, labelled Simple Bending and Modified Membrane, developed in Reference 2 and the finite element (FEM) solutions are within three, fifteen and eleven percent of the short beam shear test results, respectively.

This agreement intuitively supports the conjecture that the unstable mode II shear fracture can be associated with interlaminar shear strength. The short beam shear test, therefore, may provide definitive information that directly correlates with the mode II fracture test results. It seems to provide a simple, inexpensive means of characterizing the unstable terminal fracture process. Further substantiation of this correlation is provided by comparing photomicrographs of the short beam fracture surfaces with those generated from the unstable regions of the DCLS specimen. The fracture surfaces of the short beam appearing in Figure 14 closely resembles the unstable regions resulting from the tension and compression with little fiber breakage.

The fact that the DCLS and SCLS specimens are designed to accept reverse loading enables a simple and direct comparison between mixed-mode and mode II dominated behavior. The following points summarize the earlier observations:

1. Mode I behavior is stable and progressive, while mode II fracture is sudden, unstable and catastrophic with no apparent warning. Also, it appears to be the terminal process in stable, mixed mode fracture as well.

2. Mixed mode behavior gradually changes character with decreasing mode I contribution. The critical energy release rate for the onset of damage growth increases and post critical resistance increases for decreasing mode I contribution. The unstable character associated with decreasing mode I contribution provides a plausible reason for the increase in data scatter for specimen geometry and configuration corresponding to a higher mode II contribution [9, 10].

3. As mixed mode fracture progresses, it is clear that an abrupt transition occurs at terminal fracture. This is readily observable while conducting the tests and studying the fracture surfaces. This mode switch or transition is similar to buckling mode changes that can occur in structures. One buckling mode becomes more likely than another at a given value of the appropriate loading parameter, so a transition to a new mode occurs. For the situation at hand, it appears that the mixed mode is replaced by a (nearly) pure mode II fracture at terminal failure.

4. It appears useful to consider that fracture can occur by two distinct modes - - - a stable mixed mode fracture mode and an unstable mode II fracture mode. One limit of the mixed mode case is pure mode I. The two modes appear to be distinct, with the difference being reflected in the post critical behavior and the nature of the fracture surfaces. The mixed mode fracture surface is "hackled" in the usual way which reflects a fracture mechanism associated with resin

cleavage. On the other hand, mode II fracture is a shear fracture, as would be expected.

## CONCLUSIONS

Interlaminar fracture of the AS4/3502 graphite/epoxy material sysem has been investigated using a newly designed DCLS specimen and a SCLS specimen. A fracture toughness data base is provided through testing. A fundamental feature of the specimens is their ability to accept reverse loading . . . tension and compression testing can be performed using the same specimen (such as fatigue under alternating stresses). The specimens exhibit mixed-mode or mode II behavior, depending on the loading direction. The experimental results confirm that the specimens and tests perform as designed. Of particular interest are the findings that (1) the AS4/3502 material system shows increasing resistance to crack growth in tension, (2) fracture under tension is a three stage process . . . initiation, stable growth following a nearly linear resistance curve and a tertiary unstable terminal fracture at a high level of load, (3) the compressively loaded specimens exhibited absolutely no stable crack growth; failure occurred in a catastrophic, unstable manner with no warning at a high level of load, (4) the loads corresponding to failure by unstable fracture under tensile and compressive loadings are close to the same, (5) this fact and the similarity between the fracture surfaces in the unstable regions under tension and compression, suggest that unstable fracture is a mode II induced phenomena and (6) the unstable fracture processes at high loads may be described by strength-related parameters. It may be possible that a failure criterion rather than a crack growth or fracture mechanics-type criterion is more appropriate for the unstable, mode II. A preliminary assessment of this issue has been made through correlation with short beam shear strength data and comparisons of the fracture surfaces from short beam shear and DCLS specimen tests.

Finally, mixed mode or mode II dominated behavior associated with tension and compression testing implies that fracture can occur by two distinct modes. A stable mixed fracture mode and an unstable mode II fracture mode. The lower limit of the mixed mode case is pure mode I. The two modes appear to be distinct, with the difference being reflected in the fracture behavior and the nature of the fracture surfaces.

## ACKNOWLEDGEMENTS

The authors acknowledge the assistance of Mahera Philobos and Freddy Weinstein in conducting the experiments.

## REFERENCES

1. Armanios, E.A., Rehfield, L. W. and Reddy, A.D., "Design Analysis and Testing for Mixed-Mode and Mode II Interlaminar Fracture of Composites," presented at the 7th Symposium on Composite Materials: Testing and Design, Philadelphia, Pennsylvania, April 2-4, 1984.

2. Armanios, E.A., "New Methods of Sublaminate Analysis for Composite Structures and Applications to Fracture Processes," Ph.D. thesis, Georgia Institute of Technology, March 1985.

3. Wilkins, D.J., "A Comparison of the Delamination and Environmental Resistance of a Graphite-Epoxy and a Graphite-Bismaleimide," Technical Report NAV-GD-0037, September (1981).

4. Roderick, G.L., Everett, R.A. and Crews, J.H., Jr. "Debond Propagation in Composite-Reinforced Metals," Fatigue of Composite Materials, ASTM STP 569, 1975, pp. 295-306.

5. Paris, P.C. and Sih, G. C. in Fracture Toughness Testing, ASTM STP 381, 1970.

6. Russell, A.J. and Street, K.N., "Moisture and Temperature Effects on the Mixed-Mode Delamination Fracture of Unidirectional Graphite/Epoxy," ASTM Symposium on Delamination and Debonding of Materials, November 8-10, (1983), Pittsburgh, Pennsylvania. To appear in Delamination and Debonding of Materials , edited by W. S. Johnson, an ASTM STP Volume.

7. "Apparent Horizontal Shear Strength of Reinforced Plastics by Short Beam Method," ASTM D2344-72.

8. Whitney, J.M., "On Interlaminar Beam Experiments for Composite Materials," Tenth Annual Mechanics of Composites Review Sponsored by the Materials Laboratory, October 15-17, (1984), Dayton, Ohio, pp. 151-158.

9. O"Brien, T.K., "Mixed-Mode Strain-Energy Release Rate Effects on Edge Delamination of Composites," Effects of Defects in Composite Materials," ASTM STP 836, 1984, pp. 125-142.

10. O'Brien, T.K., "Interlaminar Fracture of Composites," NASA Technical Memorandum 85768, USAAVSCOM TR-84-B-2, June 1984.

Table 1. Summary of Experimental Data on Double Cracked-lap-shear Specimens

| Specimen Number | $P_c$ | | $(dC/da) \times 10^8$ | | $G_c$ | |
|---|---|---|---|---|---|---|
| | (N) | (LB) | (M/J) | (IN/LB IN) | ($J/M^2$) | (IN LB/$IN^2$) |
| DL-1(T) | 53379 | (12000) | 1.411 | (6.277) | 396.7 | (2.265) |
| DL-2(T) | 48753 | (10960) | 1.470 | (6.540) | 343.8 | (1.963) |
| DL-3(T) | 49731 | (11180) | 1.481 | (6.590) | 360.6 | (2.059) |

Table 2. Summary of Experimental Data on Single Cracked-lap-shear Specimens

| Specimen Number | $P_c$ | | $(dC/da) \times 10^8$ | | $G_c$ | |
|---|---|---|---|---|---|---|
| | (N) | (LB) | (M/J) | (IN/LB IN) | ($J/M^2$) | (IN LB/$IN^2$) |
| SL-2(T) | 67613 | (15200) | 1.240 | (5.515) | 558.0 | (3.186) |
| SL-3(T) | 28113 | (6320) | 1.125 | (5.003) | 87.6 | (0.500) |
| SL-4(T) | 56226 | (12640) | 1.230 | (5.472) | 383.4 | (2.189) |

Table 3. Summary of Test Results

| Specimen Code | $\varepsilon_c$ (Micro MM/MM) | $\varepsilon_f$ (Micro MM/MM) | $P_c$ N | $P_c$ (LBS) | $P_f$ N | $P_f$ (LBS) | $G_c$ J/N$^2$ | $G_c$ (LB IN/IN$^2$) | $G_f$ J/M$^2$ | $G_f$ (LB IN/IN$^2$) |
|---|---|---|---|---|---|---|---|---|---|---|
| SL-1(C) | 5160 | 5160 | 82381 | (18520) | 82381 | (18520) | 808.210 | (4.615) | 808.210 | (4.615) |
| SL-2(T) | 4249 | 5686 | 67613 | (15200) | 90477 | (20340) | 557.954 | (3.186) | 999.099 | (5.705) |
| SL-3(T) | 1768 | 5063 | 28113 | (6320) | 80513 | (18100) | 87.563 | (0.500) | 718.545 | (4.103) |
| SL-4(T) | 3528 | 4712 | 56226 | (12640) | 75086 | (16880) | 383.528 | (2.190) | 684.045 | (3.906) |
| SL-5(C) | 4810 | 4810 | 76598 | (17220) | 76598 | (17220) | 710.139 | (4.055) | 710.139 | (4.055) |
| SL-6(C) | 5228 | 5228 | 82737 | (18600) | 82737 | (18600) | 693.502 | (3.960) | 693.502 | (3.960) |
| DL-1(T) | 3283 | 4868 | 53379 | (12000) | 79178 | (17800) | 396.662 | (2.265) | 871.957 | (4.979) |
| DL-2(T) | 3086 | 4335 | 48753 | (10960) | 68503 | (15400) | 343.774 | (1.963) | 678.967 | (3.877) |
| DL-3(T) | 3101 | 4156 | 49731 | (11180) | 66634 | (14980) | 360.586 | (2.059) | 647.444 | (3.697) |
| DL-4(C) | 3965 | 3965 | 64499 | (14500) | 64499 | (14500) | 581.771 | (3.322) | 581.771 | (3.322) |
| DL-7(C) | 4784 | 4784 | 77666 | (17460) | 77666 | (17460) | 857.246 | (4.895) | 857.246 | (4.895) |
| DL-8(C) | 4924 | 4924 | 80068 | (18000) | 80068 | (18000) | 995.946 | (5.687) | 995.946 | (5.687) |

$E_{effective}$ = 50.332 GPa (7.300 Msi)

("c" denotes starting critical value, "f" denotes final or failure)

Table 4. Comparison of Interlaminar Shear Data

| Specimen | Failure Load | | Maximum Shear Stress/Shear Strength | | | | | |
|---|---|---|---|---|---|---|---|---|
| | | | Simple Bending | | Modified Membrane | | FEM | |
| | N | (LBS) | MPa | (Psi) | MPa | (Psi) | MPa | (Psi) |
| **A. Fracture Test** | | | | | | | | |
| DL-1(T) | 79,178 | (17,800) | 57.351 | (8,318) | 50.208 | (7,282) | 52.648 | (7,636) |
| DL-2(T) | 68,503 | (15,400) | 49.622 | (7,197) | 43.437 | (6,300) | 45.547 | (6,606) |
| DL-3(T) | 66,634 | (14,980) | 48.270 | (7,001) | 42.251 | (6,128) | 44.306 | (6,426) |
| DL-4(C) | 64,499 | (14,500) | 46.719 | (6,776) | 40.900 | (5,932) | 42.885 | (6,220) |
| DL-7(C) | 77,666 | (17,460) | 56.261 | (8,160) | 49.249 | (7,143) | 51.642 | (7,490) |
| DL-8(C) | 80,068 | (18,000) | 57.999 | (8,412) | 50.773 | (7,364) | 53.241 | (7,722) |
| | | Mean | 52.704 | (7,644) | 46.133 | (6,691) | 48.381 | (7,017) |
| **B. Short Beam Three Point Bending Test** | | | | | | | | |
| DL-3(T)-1 | 4,559 | (1,025) | 47.091 | (6,830) | | | | |
| DL-3(T)-2 | 4,982 | (1,120) | 55.820 | (8,096) | | | | |
| DL-4(C)-1 | 4,693 | (1,055) | 46.560 | (6,753) | | | | |
| DL-4(C)-2 | 5,894 | (1,325) | 53.097 | (7,701) | | | | |
| DL-7(C)-1 | 6,058 | (1,362) | 60.557 | (8,783) | | | | |
| DL-8(C)-1 | 5,716 | (1,285) | 59.481 | (8,627) | | | | |
| DL-8(C)-2 | 5,667 | (1,274) | 57.895 | (8,397) | | | | |
| DL-8(C)-3 | 5,471 | (1,230) | 55.020 | (7,980) | | | | |
| | | Mean | 54.441 | (7,896) | | | | |

# LIST OF FIGURES

Figure

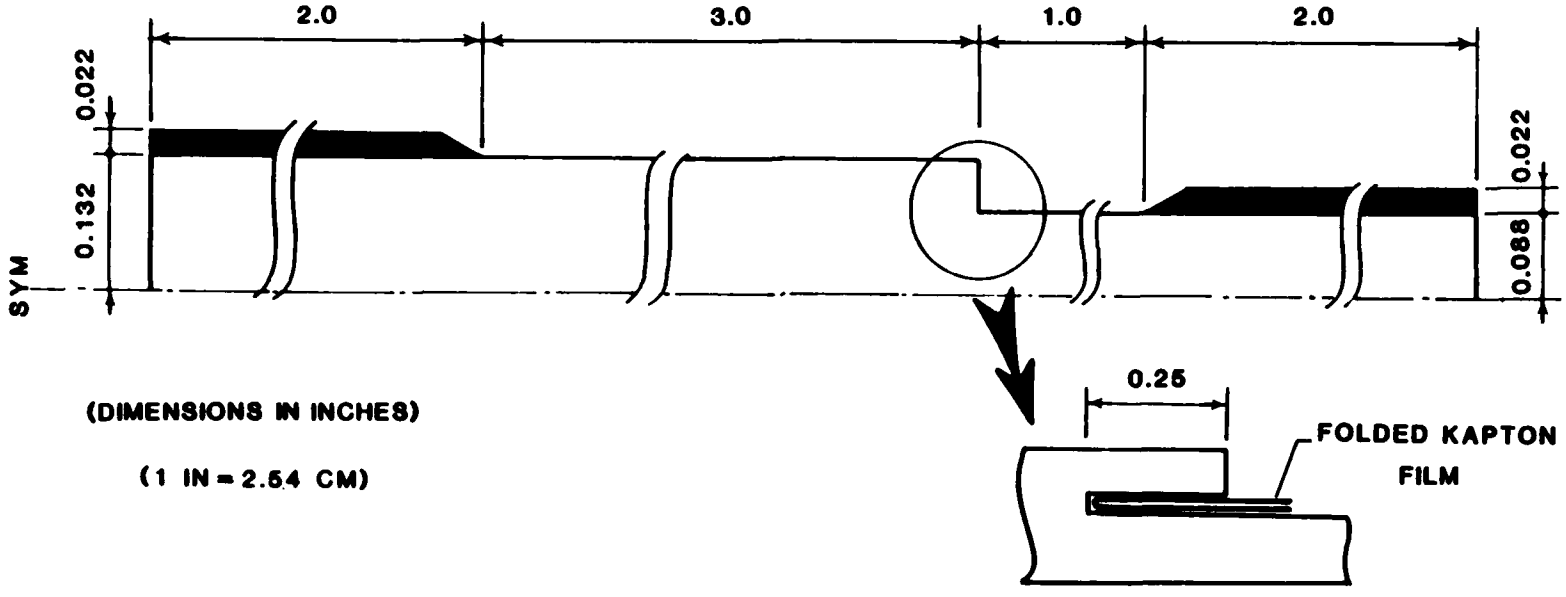
2.0
3.0
1.0
2.0
0.022
0.132
SYM
0.022
0.088
(DIMENSIONS IN INCHES)
(1 IN = 2.54 CM)
0.25
FOLDED KAPTON
FILM

FIG. 1

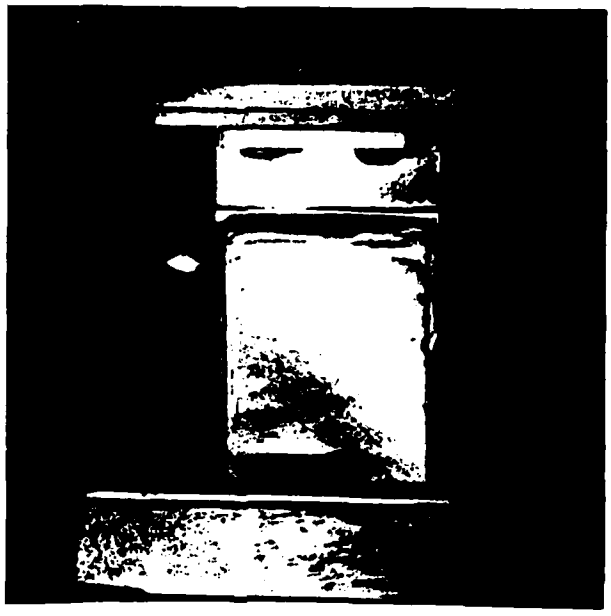

FIG.2

FIG.3

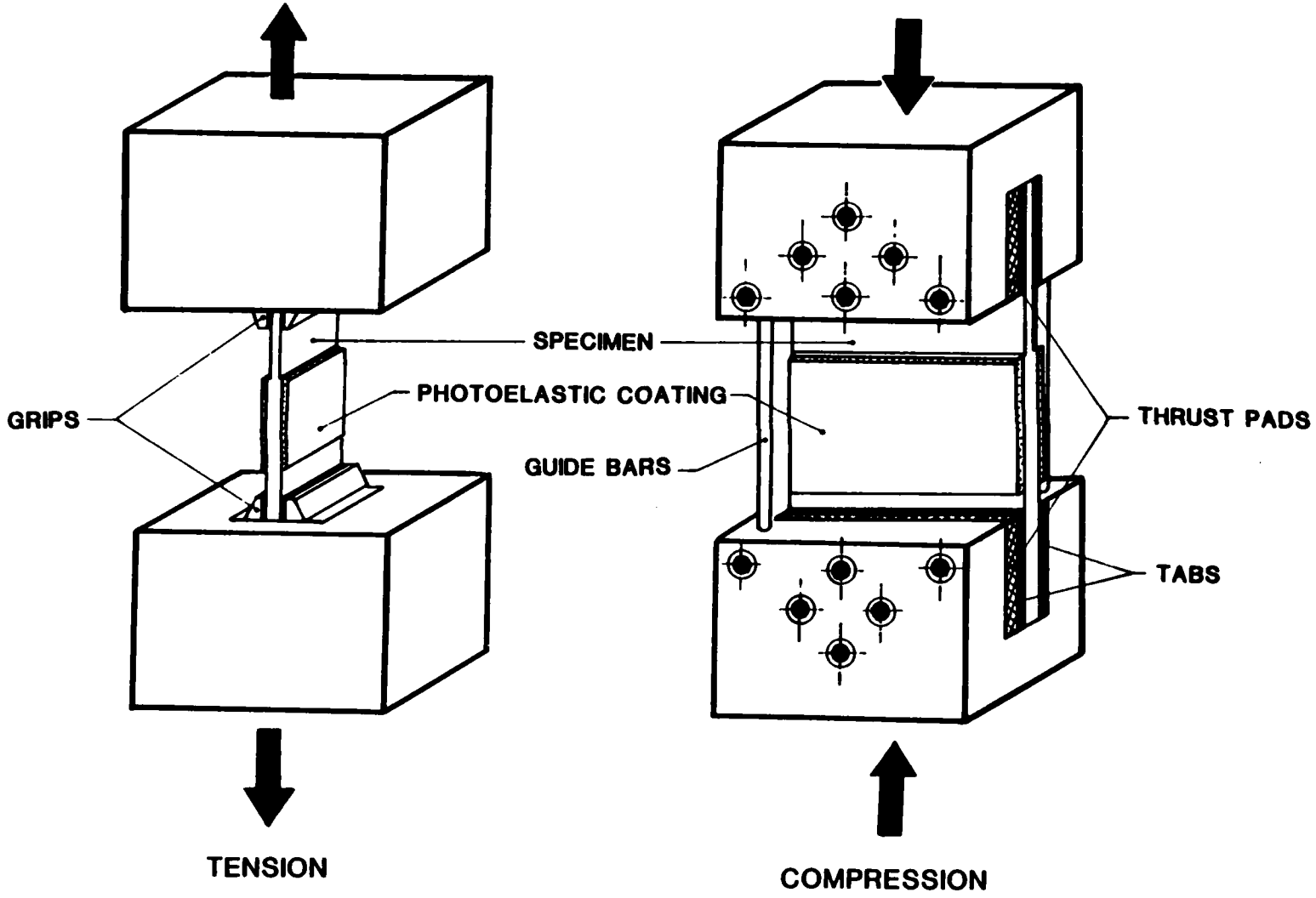
SPECIMEN
PHOTOELASTIC COATING
GRIPS
GUIDE BARS
THRUST PADS
TABS
TENSION
COMPRESSION

FIG.4

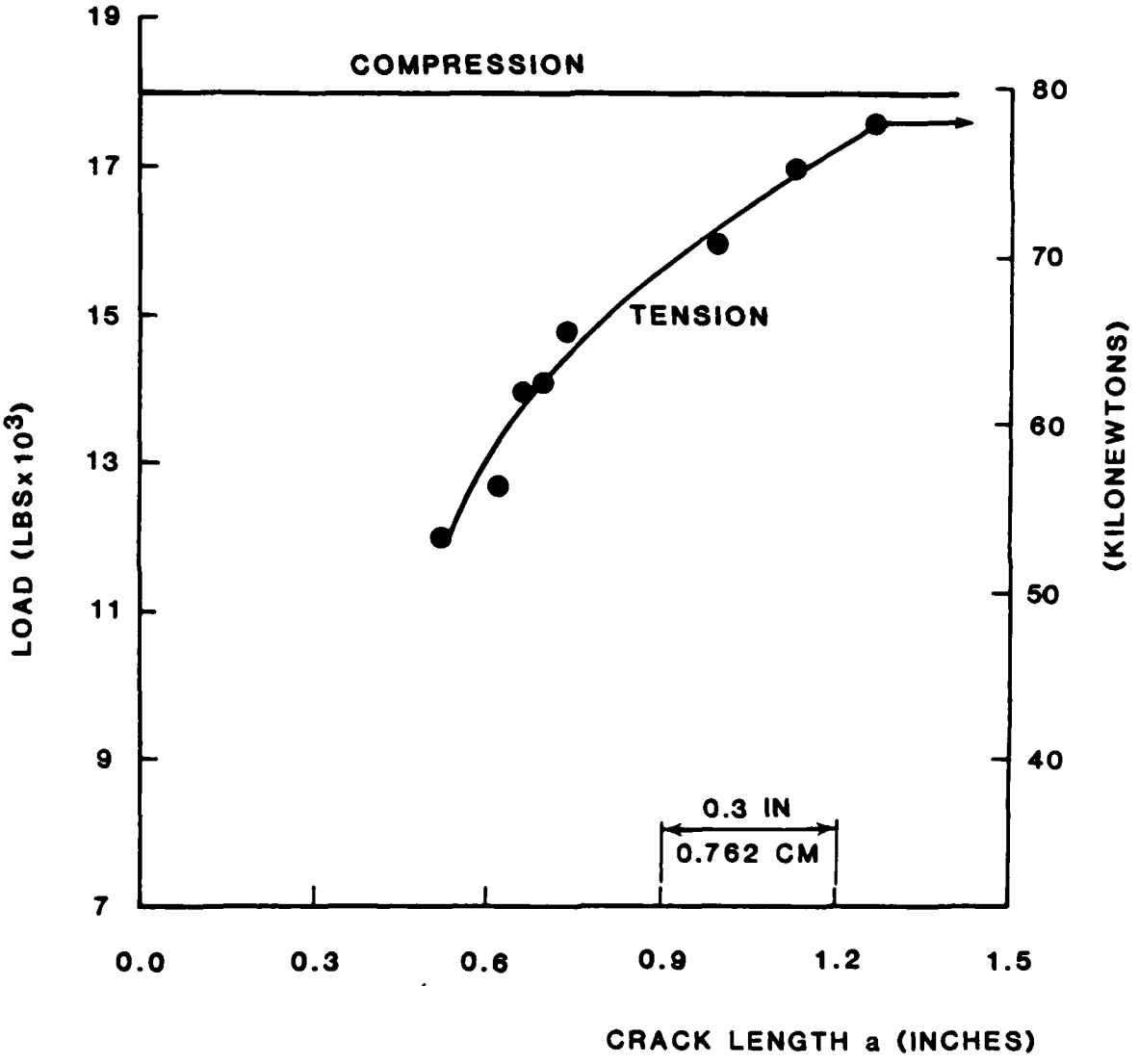
19
17
15
13
11
9
7
COMPRESSION
TENSION
80
70
60
50
40
0.3 IN
0.762 CM
LOAD (LBS x 10³)
(KILONEWTONS)
0.0
0.3
0.6
0.9
1.2
1.5
CRACK LENGTH a (INCHES)

FIG.5

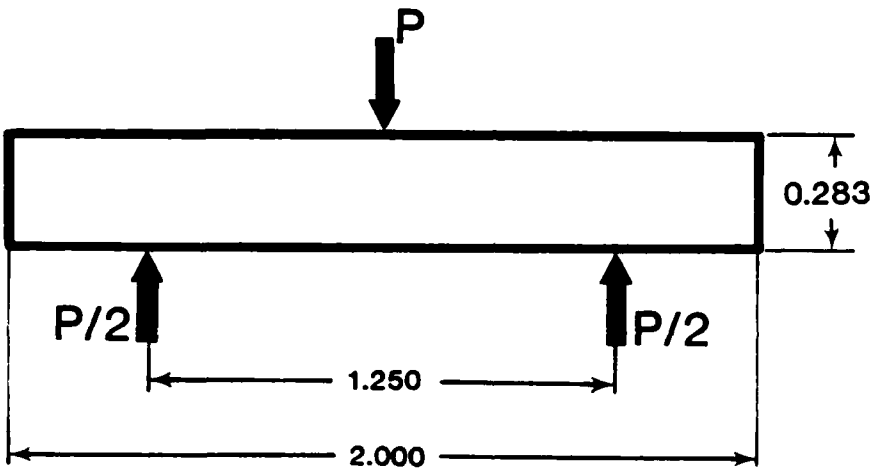


(DIMENSIONS IN INCHES)

(1 IN = 2.54 CM)

FIG.6

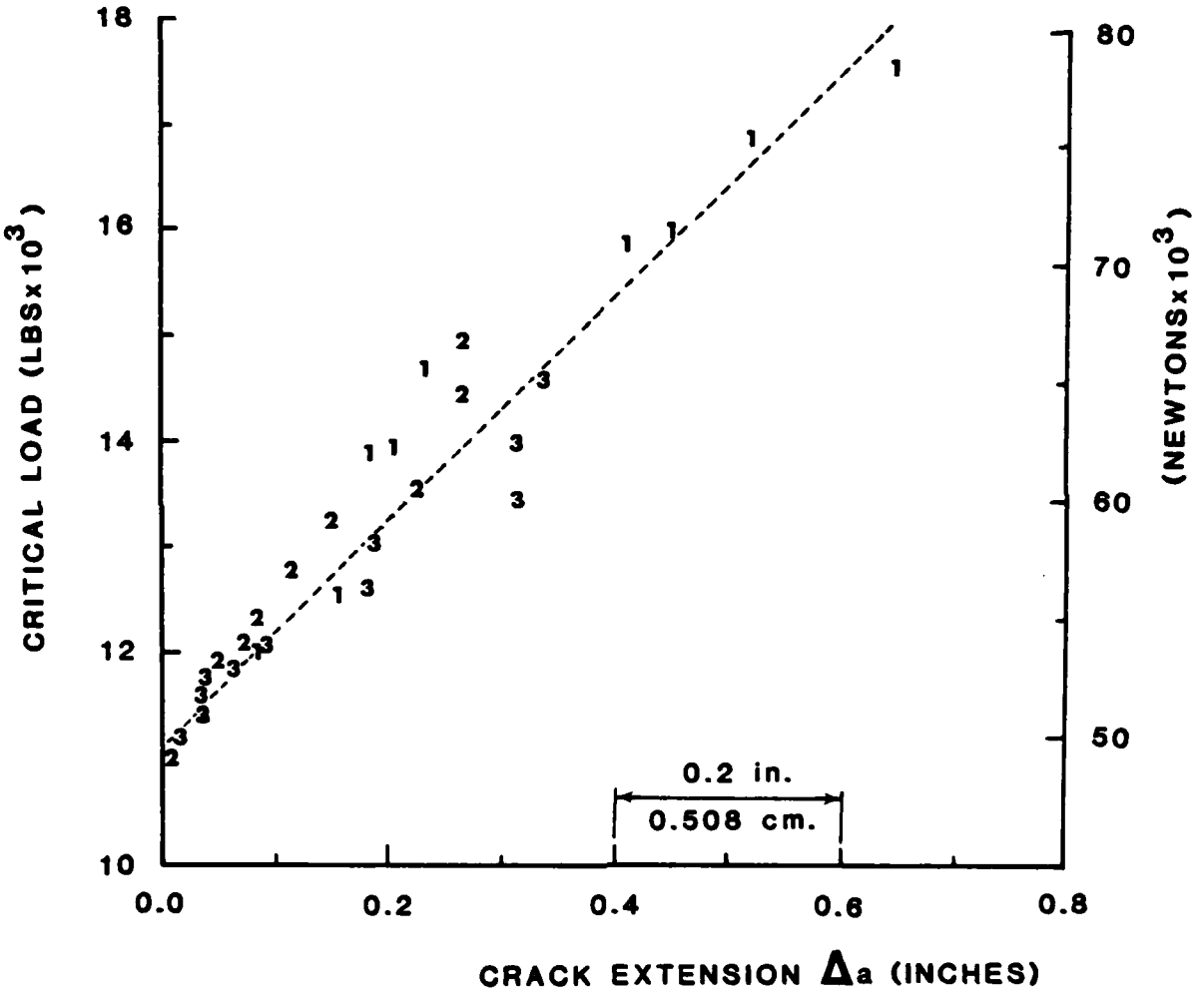
18
16
14
12
10
80
70
60
50
0.0
0.2
0.4
0.6
0.8
CRITICAL LOAD (LBS x 10^3)
(NEWTONS x 10^3)
0.2 in.
0.508 cm.
CRACK EXTENSION Δa (INCHES)

FIG.7

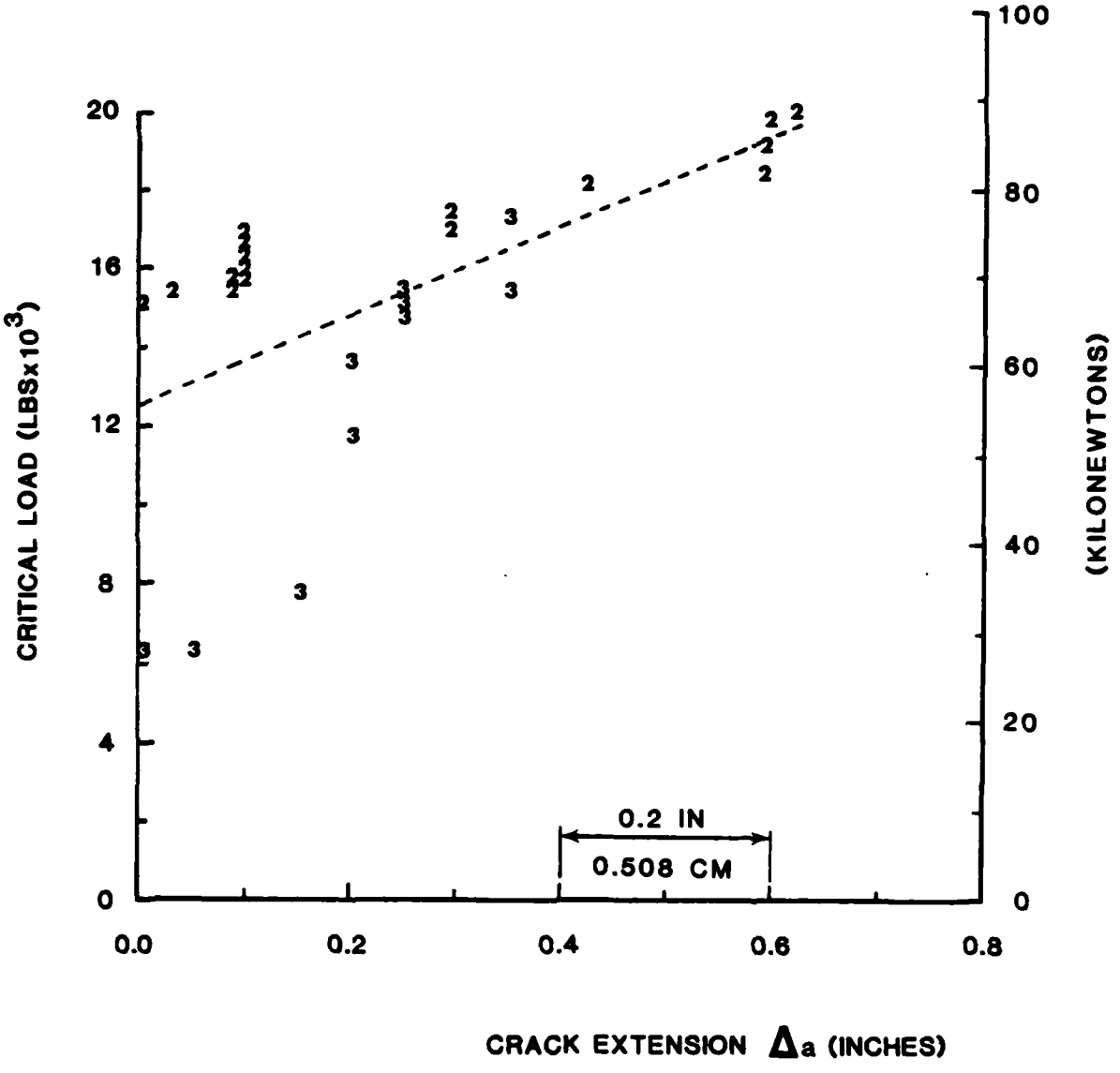
CRITICAL LOAD (LBSx10$^3$)
(KILONEWTONS)
0.2 IN
0.508 CM
CRACK EXTENSION Δa (INCHES)
0
4
8
12
16
20
0
20
40
60
80
100
0.0
0.2
0.4
0.6
0.8

FIG.8

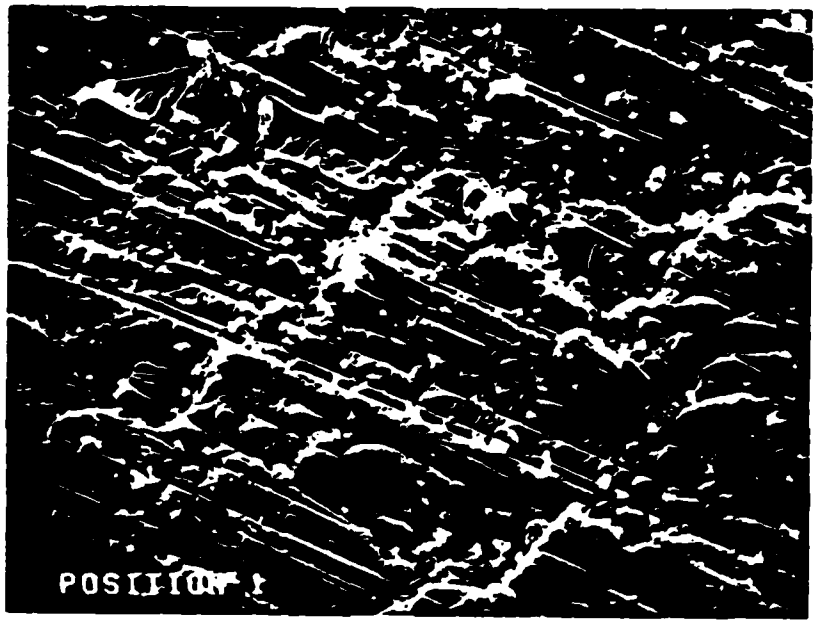

FIG.9

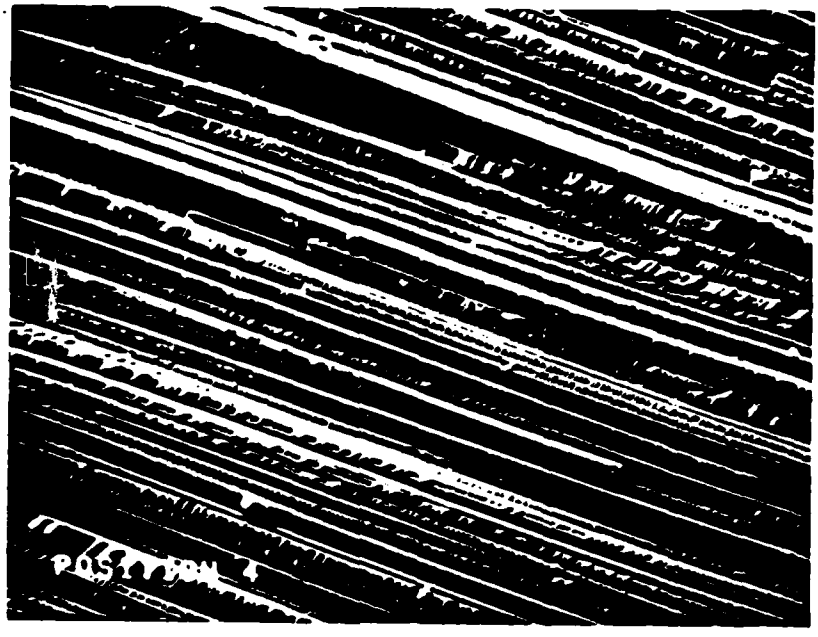

FIG.10

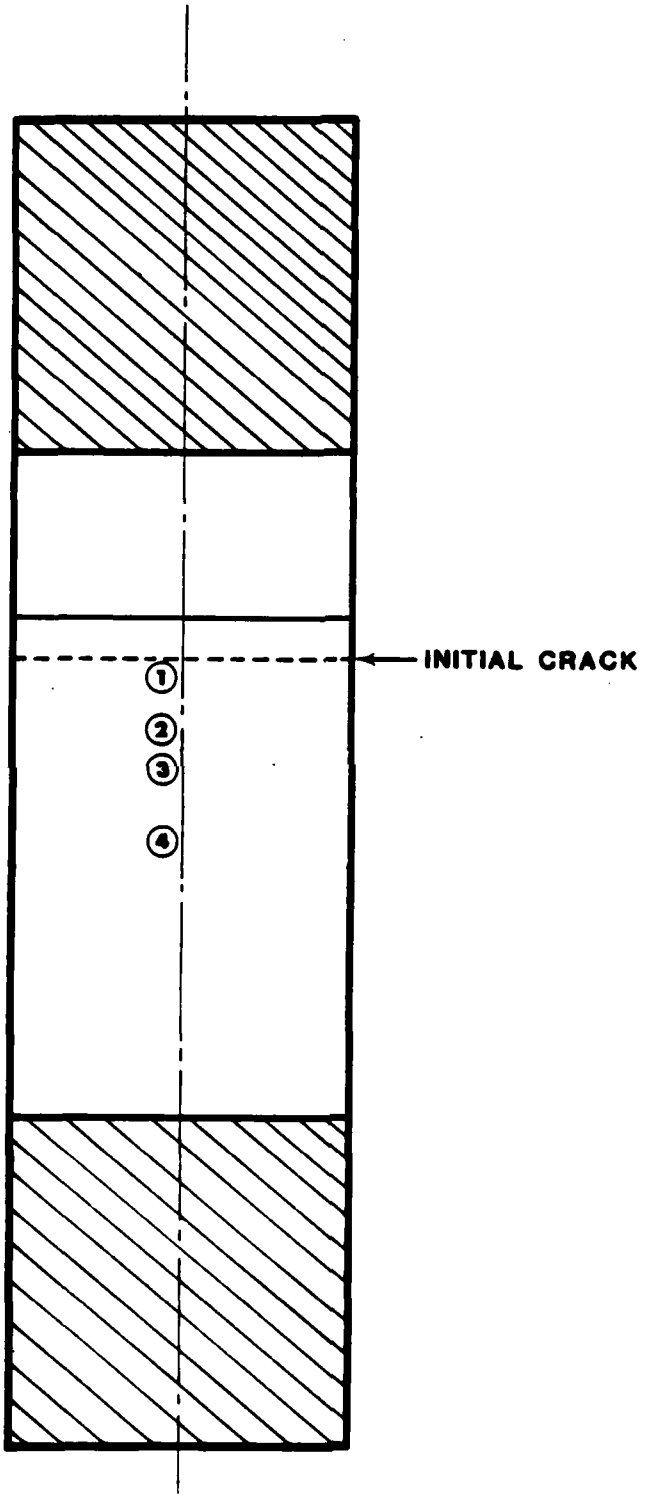


FIG. 11

TENSION

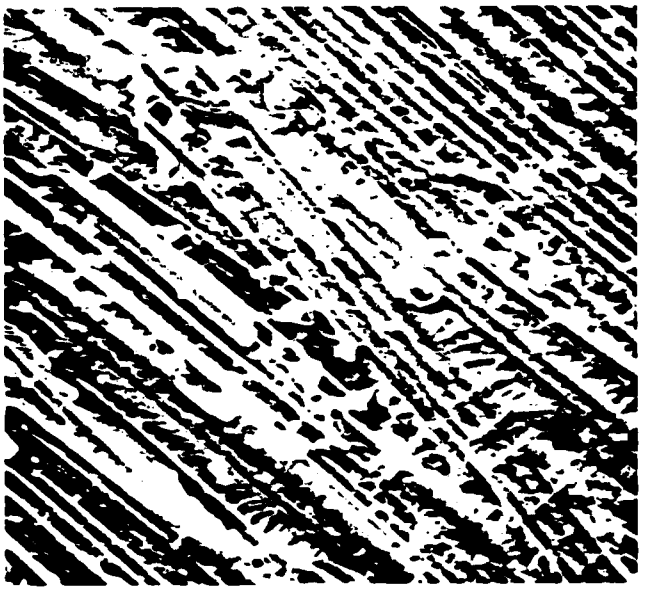

FIG. 12

← DIRECTION OF CRACK PROPAGATION

(ORIGINAL MAGNIFICATION x 400)

COMPRESSION

(ORIGINAL MAGNIFICATION x 500)

FIG. 13

UPPER SURFACE

← DIRECTION OF CRACK PROPAGATION

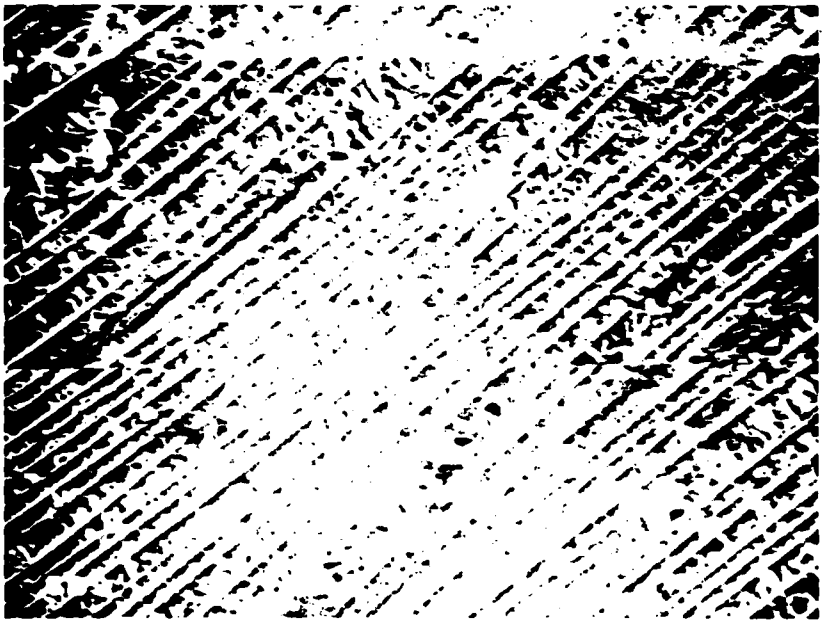

LOWER SURFACE

PHOTOMICROGRAPH OF FRACTURE SURFACE -

SHORT BEAM SHEAR SPECIMEN - ORIGINAL MAGNIFICATION x400

FIG.14

# APPENDIX II

# INTERLAMINAR FRACTURE PROCESSES IN RESIN MATRIX COMPOSITES UNDER STATIC AND FATIGUE LOADING*

A. D. Reddy, L.W. Rehfield, F. Weinstein and E.A. Armanios**
School of Aerospace Engineering
Georgia Institute of Technology
Atlanta, Georgia 30332

## EXTENDED ABSTRACT

In both static and fatigue loading situations interlaminar fracture or delamination has been observed to be a primary damage mode in laminated composites. The high interlaminar stresses in the vicinity of stress raisers are responsible for this. Efforts have been made by several investigators to determine the interlaminar fracture toughness of laminated composites using different testing approaches. One of them is the double cracked-lap-shear (DCLS) test developed at the Georgia Institute of Technology[1]. This specimen, shown in Figure 1, is designed such that both tension and compression tests can be performed on the same specimen. These tests have shown that a stable crack growth resulted under tensile loading followed by sudden failure, whereas a single, unstable, catastrophic fracture event corresponds with the specimen under compression.

The above DCLS specimen fails in a mixed mode (mode I and mode II) under tensile loading and mode II under compressive loading[2]. Through limited documentation it has been noted in literature that mode I, or the peel stress-induced failure mode, is the one that drives the delamination in bonded lap joints[3,4,5]. A similar phenomenon is anticipated in laminated composites. Hence, the first part of this experimental and analytical study focuses on the opening mode

* Work sponsored by AFOSR under Grant 83-0056 and 85-0179.

** Senior Research Engineer, Professor, Graduate Research Assistant and Research Engineer, respectively.

effects and its alleviation in order to determine its role on the fracture processes in laminated composites.

The second part of the study deals with cyclic debond growth under constant amplitude tension-tension and compression-compression fatigue loading. This is the only known compression-compression fatigue interlaminar fracture work of its kind. The threshold of delamination growth under tension-tension fatigue is observed to be lower than the static loading value. This data is generated first on the DCLS specimen fabricated out of a AS4/3502 graphite-epoxy material system. The mode I suppression methodology is used next in the fatigue loading context to study the cyclic debond growth retardation. As static compression loading on the specimen causes failure only in mode II, the compression fatigue tests are performed mainly to confirm the sudden, total failure of the specimen and also to determine the threshold levels.

The typical test setup for mode I suppression is shown in Figure 2. A calibrated C-clamp type device is used to apply the normal loading (which tends to produce compressive peel stress) on the specimen. A photoelastic coating is bonded to the lap surface of the specimen to monitor the movement of the crack front. The clamp is positioned slightly ahead of the crack front and tightened to apply a known initial normal loading. The specimen is then loaded in tension. The load at which the crack crosses the normal loading line is recorded together with the crack growth. This procedure is repeated until the laps delaminate with sudden, unstable crack growth.

The preliminary data summarized in Figure 3 indicates that mode I contribution is totally eliminated at a normal loading of 153 lb/in, which results in the applied load to increase with no crack growth until failure. The last phase of failure is similar to the compression behavior where no crack growth is observed

under increasing load until the ultimate failure load is reached. This provides a partial explanation for the effectiveness of stitching in laminates and stiffener/skin construction. The opening mode is suppressed or retarded by stitching.

The constant amplitude tension-tension fatigue test data is presented in Figure 4. The term $P_{MAX}$ denotes the maximum applied cyclic load and $P_{NSC}$ is the nominal static critical load (corresponds to the first crack growth in the static tension test). At R = 0.2 and frequency of 10 cycles/minute, a $P_{MAX}/P_{NSC} = 0.85$ did not cause the crack to grow until about 175 cycles. When this ratio was increased to 0.95 the crack grew steadily and reached an asymptotic value of 0.34 inches around 1000 cycles. This information suggests that the cyclic load threshold is lower than the static case and results in larger crack growth. The compression-compression fatigue test results in Figure 5 suggest that the specimen fails in a catastrophic manner under a $P_{MAX}/P_{ULT} = 0.9$ at 14700 cycles. The load at which the failure occurs under static compression loading is denoted by $P_{ULT}$.

This paper summarizes the experimental information and analytical results on mode I suppression and the experimental data under both compression and tension fatigue loading.

## REFERENCES


1. Armanios, E.A., Rehfield, L.W. and Reddy, A.D., "Design Analysis and Testing for Mixed Mode and Mode II Interlaminar Fracture of Composites," presented at the ASTM Symposium on Composite Materials: Testing and Design, Philadelphia, PA, April 1984.

2. Rehfield, L.W., Reddy, A.D. and Armanios, E.A., "Interlaminar Fracture of Graphite-Epoxy Composites Under Tensile and Compressive Loading," presented at the ASTM Symposium on Toughened Composites, Houston, Texas, March 1985.

3. Everett, R.A., Jr., "The Role of Peel Stresses in Cyclic Debonding," nASA TM 84505, June 1982.

4. Mall, S., Johnson, W.S., and Everett, R.A., Jr., "Cyclic Debonding of Adhesively Bonded Composites," NASA TM 84577, November 1982.

5. O'Brien, T.K., "Interlaminar Fracture of Composites," NASA TM 85768, June 1984.

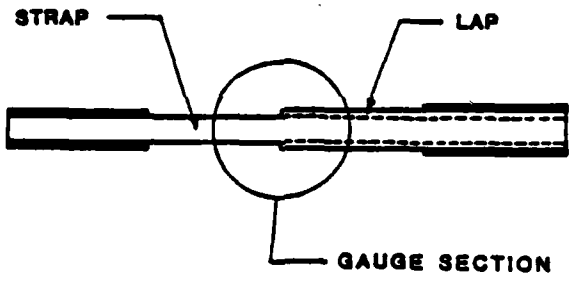


Figure 1. The Double Cracked-Lap-Shear Specimen

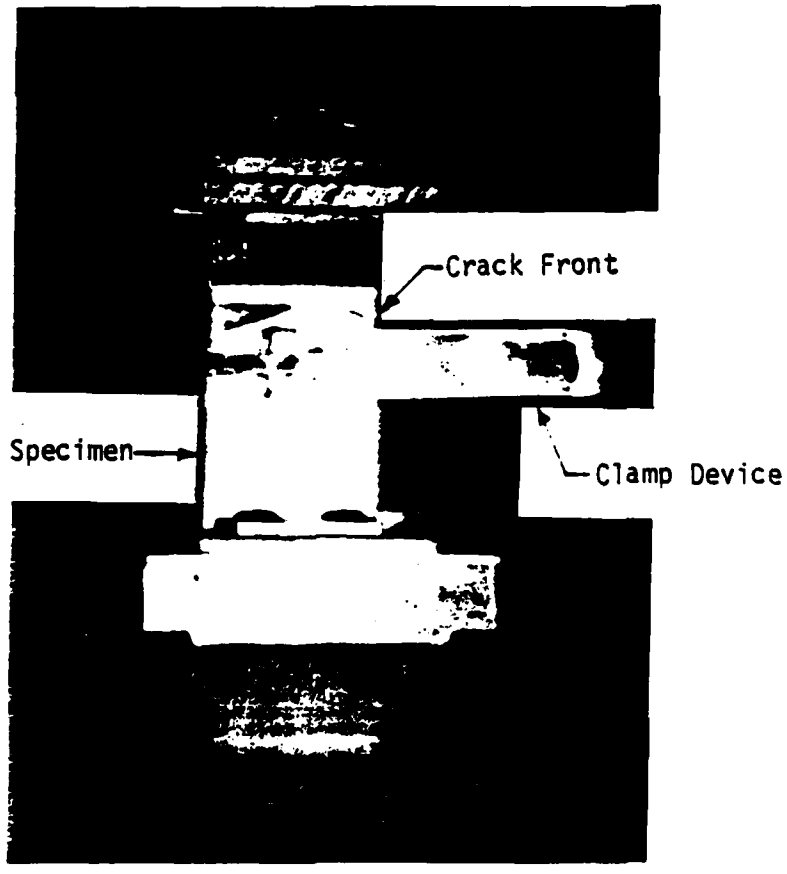


Figure 2. Typical Experimental Setup

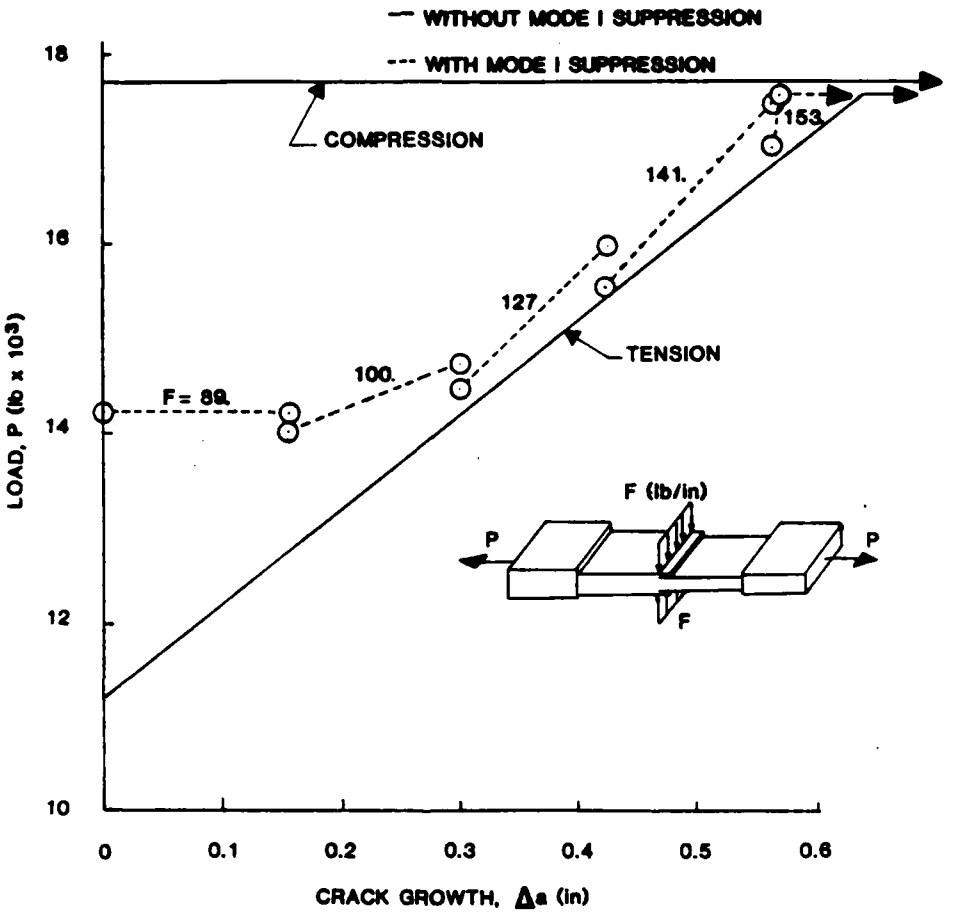


Figure 3. Comparison of Crack Growth Resistance Data With and Without Mode I Suppression

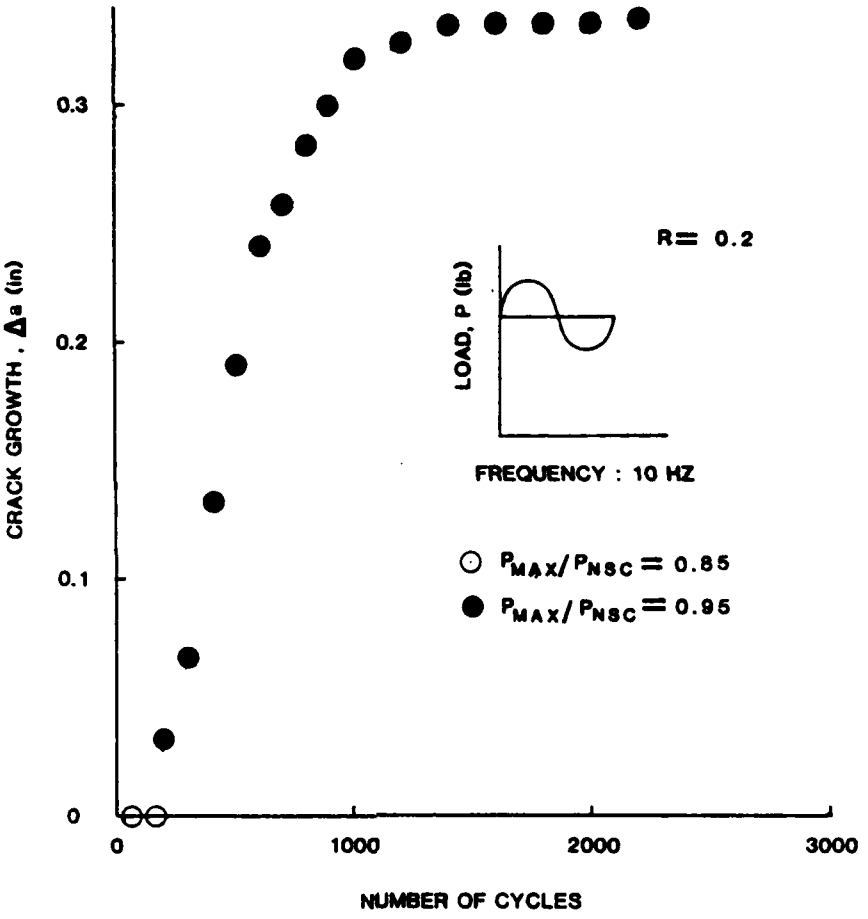


Figure 4. Tension-Tension Fatigue Crack Growth Results

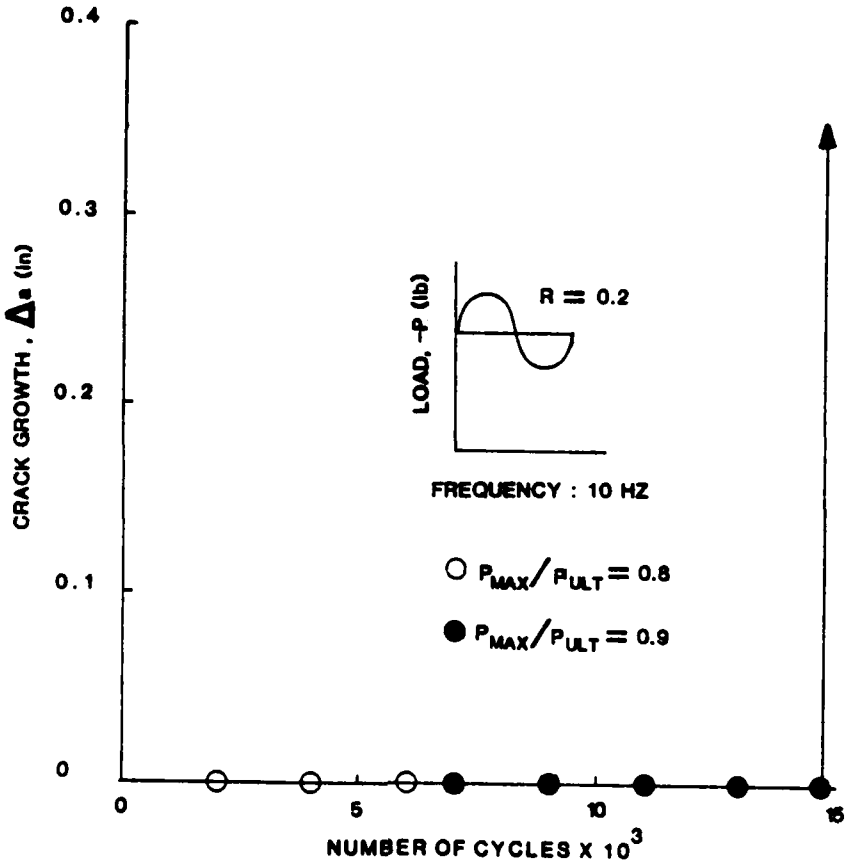


Figure 5. Compression- Compression Crack Growth Results

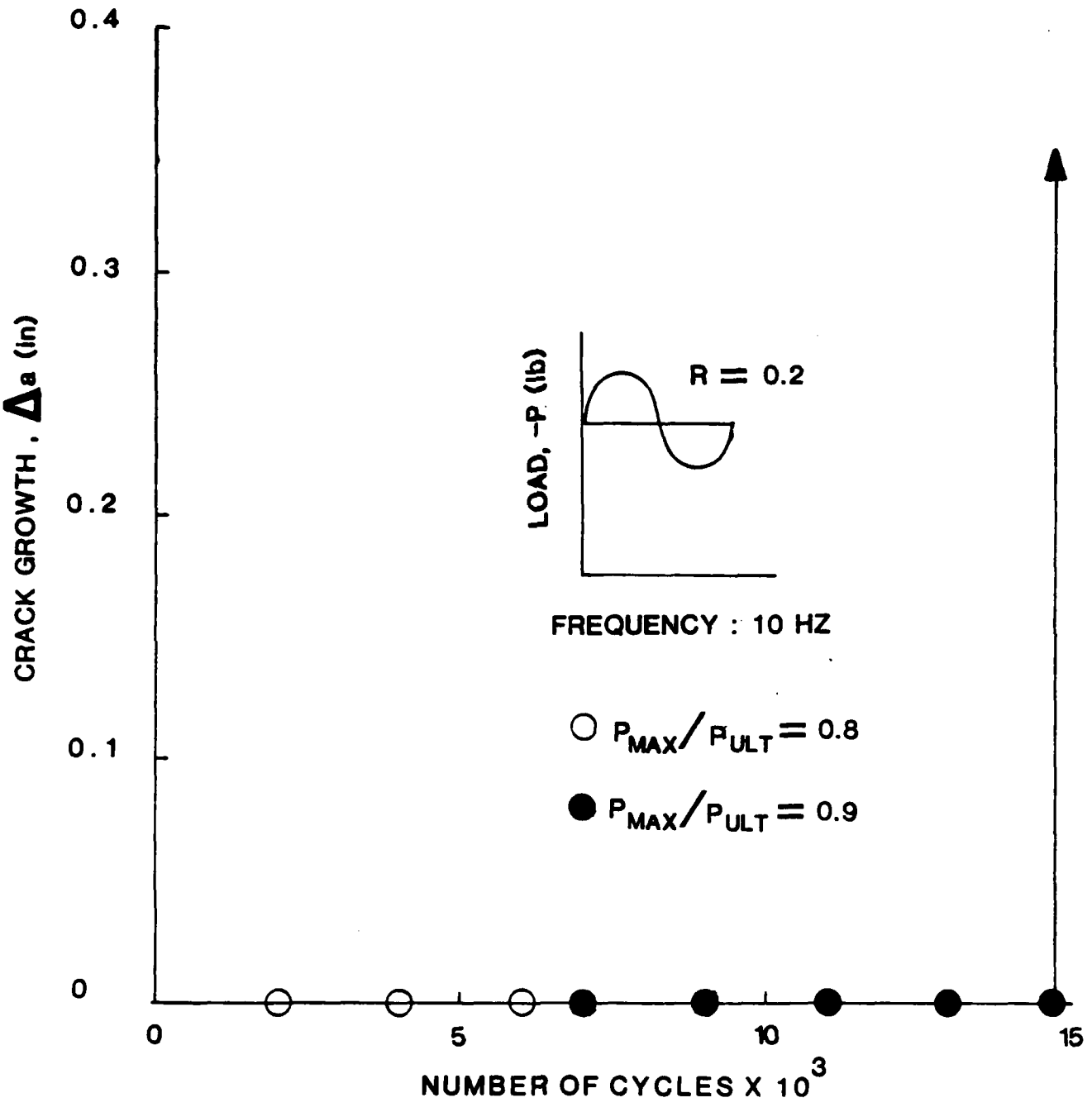


Figure 5. Compression-Compression Crack Growth Results

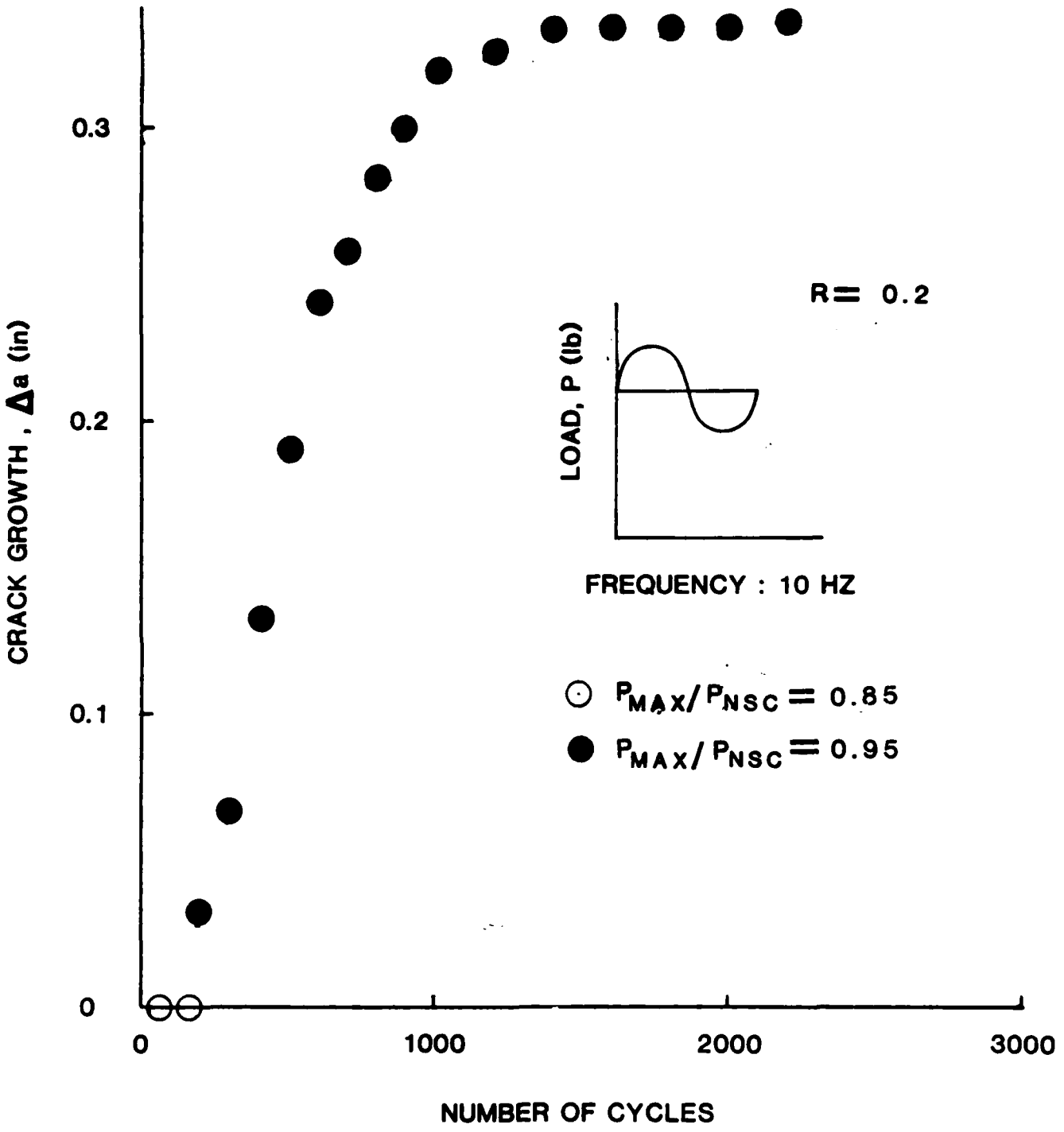


Figure 4. Tension-Tension Fatigue Crack Growth Results

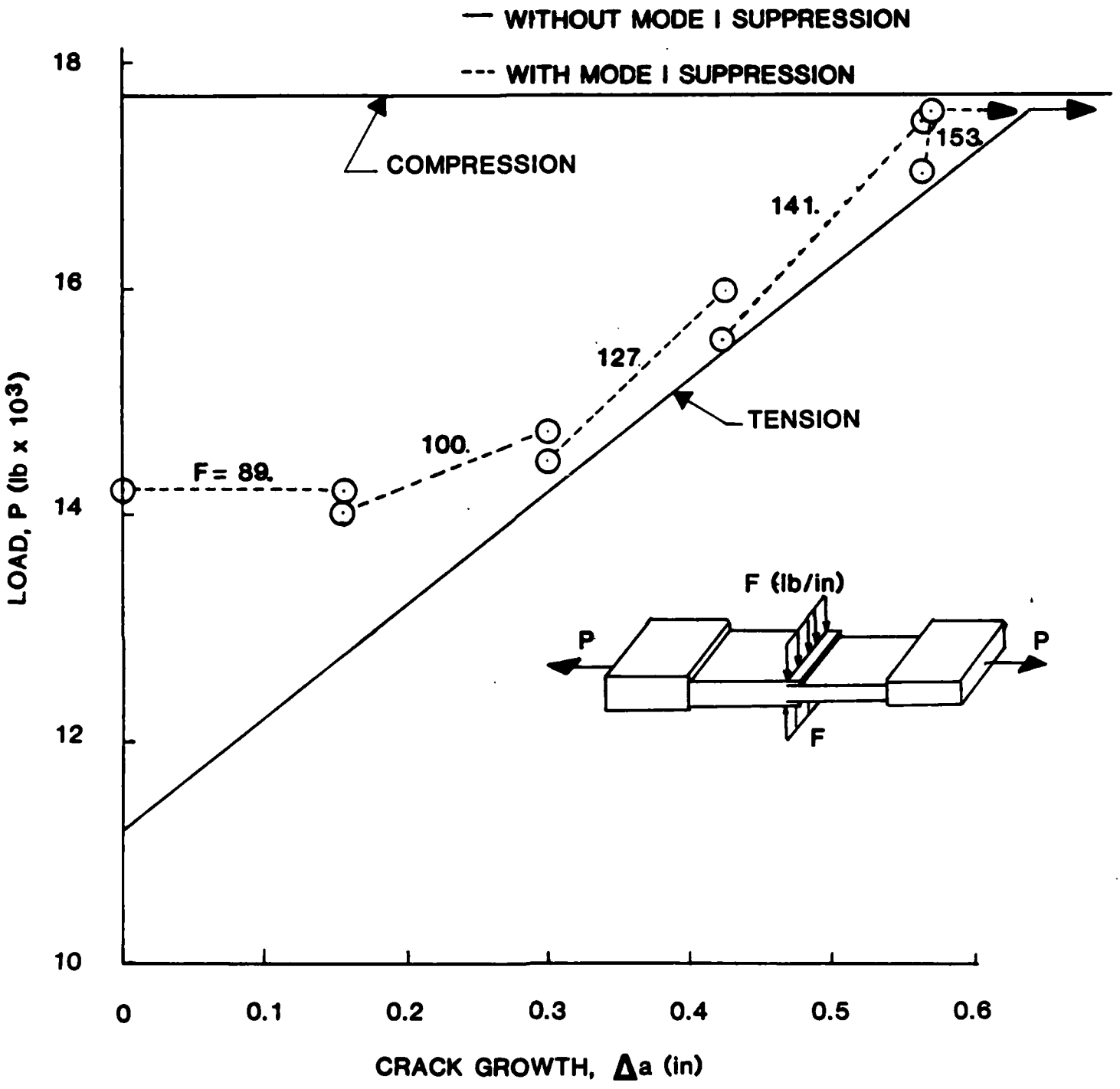


Figure 3. Comparison of Crack Growth Resistance Data With and Without Model Suppression

# END

# FILMED

1-86

# DTIC